Journal of Sound and Vibration (1998) **216**(3), 461–493
Article No. sv981710

THE ACOUSTIC RADIATION OF BAFFLED FINITE DUCTS WITH VIBRATING WALLS

A. H. W. M. KUIJPERS

Faculty of Mechanical Engineering, Eindhoven University of Technology, P.O. Box 513, 5600 *MB Eindhoven, The Netherlands*

S. W. RIENSTRA

Faculty of Mathematics and Computing Science, Eindhoven University of Technology, P.O. Box 513, 5600 *MB Eindhoven, The Netherlands*

AND

G. VERBEEK AND J. W. VERHEIJ

Faculty of Mechanical Engineering, Eindhoven University of Technology, P.O. Box 513, 5600 *MB Eindhoven, The Netherlands*

(*Received* 23 *October* 1997, *and in final form* 28 *April* 1998)

A mathematical model for the radiation of baffled finite ducts is presented. This model was developed to be used for the design process of Magnetic Resonance Imaging (MRI) scanners. The added value of utilizing this model over using general purpose acoustics software is the increased insight into the acoustic phenomena in the baffled finite duct and the increased efficiency. The problem domain of the scanner was characterized as a finite duct with infinite flanges, acoustically excited by wall vibration. A mathematical model for this problem domain was developed, based on a model description of the acoustic field. The model was constructed by using a Fourier transformation technique for the Helmholtz equation and the velocity boundary conditions at the duct's wall. The diffraction of sound at the flanges was described with reflection coefficients. Two simultaneous matrix equations were found describing the acoustic field in the wall-driven baffled finite duct. Special attention was paid to the efficient implementation of the model. The physical and computational characteristics of the model were determined by parameter study and by comparison with Fourier Boundary Element Method (BEM) models of the MRI scanner. A good agreement was found between the results obtained with the baffled duct and the Fourier BEM models. Because of the direct relationship between design parameters and acoustic response, and because of the better numerical efficiency of the baffled duct model as opposed to the Fourier BEM models, the application of the baffled duct model in the design process is viable.

1. INTRODUCTION

In contemporary acoustic engineering it is becoming more and more common to use general purpose acoustics software based on the Finite Element Method

0022–460X/98/380461 + 33 $30.00/0

(FEM) or Boundary Element Method (BEM) in the design process of complex structures. With the ever increasing computational power of modern computers and maturation of the acoustic software, the usage of these programs will certainly increase. But the methods normally used in these programs have a major drawback: you only get numbers, not insight. An acoustic engineer has to relate design changes to acoustic response changes, but the methods used in these programs do not offer this relationship directly; it is often a matter of engineering experience to interpret the numbers to obtain insight. This problem can be tackled by the development of problem domain specific tools. In these tools the geometry of the acoustic domain is restricted, but through this simplification a much better understanding of the acoustical phenomena in that domain is gained, possibly together with an increased efficiency. The benefits of this approach will be presented here with the development of a mathematical model for the acoustic radiation of a Magnetic Resonance Imaging (MRI) scanner.

An MRI scanner is used for medical imaging of human body internals in arbitrary direction (see, e.g., reference [1]). It is especially suited for soft tissue imaging. A well known problem of MRI-scanners is the fact that during the imaging process both patient and operator are exposed to high noise levels (up to 90–100 dB), mainly caused by the vibration of the so-called gradient coils (see Figure 1). The development of new MRI imaging techniques brings about even higher noise levels and it is recognized that a substantial decrease of the noise production of the scanner can only be achieved by explicitly incorporating the acoustic behavior of the gradient coils into the design phase (see, e.g., reference [2]). However, this is far from straightforward because of the large dimensions of the MRI scanner and the complexity of the vibration of the gradient coils, which necessitates large modelling and computational efforts using general purpose acoustic tools.

A good model for the acoustic behavior of the MRI scanner and its gradient coils must incorporate two aspects: the specific geometry of the scanner and its

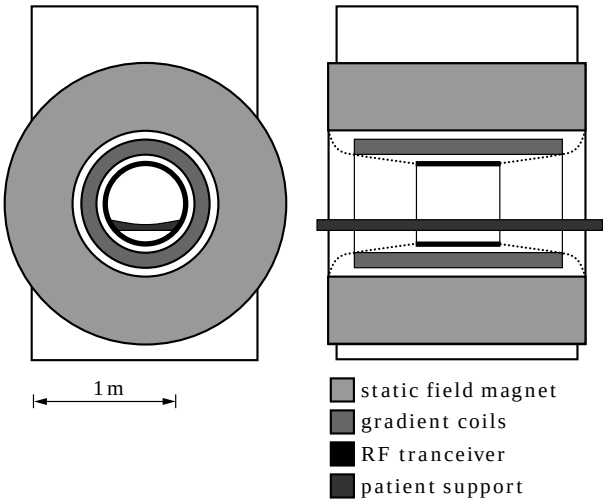

Figure 1. Schematic front view and cross-section of an MRI-scanner.

complex acoustic boundary conditions. As a first approximation, the geometry of the scanner can be modelled as being axisymmetric. Secondly, the boundary conditions can be approximated by assuming that only the gradient coil (duct wall) can vibrate and thus radiate acoustic energy.

Modelling the acoustic behavior of the MRI scanner with rather general techniques such as the three dimensional acoustic Boundary Element Method (3d-BEM) is not feasible because of the huge computational requirements that are involved, despite the model simplifications. A significant reduction in computational effort can be realized by utilizing the so-called Fourier-BEM which exploits the axisymmetric properties of the geometry without requiring axisymmetric boundary conditions [3–5]. This is accomplished by using a Fourier series expansion of the acoustic variables in circumferential direction and hence reducing the dimensionality of the problem by one. But similar to the 3d-BEM, it does not offer directly a relationship between design parameters for the MRI-scanner (like the scanner's inner radius, or its length) and its acoustic response parameters (like inner-duct pressure or radiated power).

Increased insight and a further model reduction can be achieved if the central part of the MRI scanner with its gradient coils can be approximated as a finite duct (constant cross-section) with infinite flanges. This way, it is possible to use duct acoustics theory which receives considerable attention in the basic acoustic textbooks [6–9]. The theory presented in these books is, however, not sufficient to model the MRI-scanner; it generally only deals with (semi-)infinite ducts and a plane wave approximation for the acoustic field inside the duct.

To the authors' knowledge, no studies have been reported in the literature dealing with the duct acoustics of a finite duct with vibrating walls. Models for the propagation and diffraction of sound inside semi-infinite and finite ducts, have been reported (see, e.g., references [10–14]) but they were mainly dealing with the radiation of (point) sources or only propagation of sound inside hard-walled ducts, not with vibrating walls. Studies in the literature of the sound radiation of cylinders with vibrating walls (see, e.g., references [15–20]) all deal with external radiation, not internal. Nevertheless, these models were useful as they provided the building blocks for an accurate and efficient acoustic model for the MRI scanner based on duct acoustics that will be presented here.

The model for the radiation of sound inside a baffled finite duct with vibrating walls, presented here, is an extension of the model presented by Doak [11] for the radiation of sound by a distribution of sources inside a finite length hard-walled duct with infinite flanges. The model's impedance boundary conditions in the duct at the flanges are handled with so-called reflection coefficients [12]. Special attention was paid to the computational efficiency of the model and therefore an alternative for computation of these reflection coefficients is presented. The coupling between the reflection coefficients at the duct's exists and the sound field created in and propagated through the finite duct is expressed by two matrix equations that need to be solved simultaneously or iteratively. The physical and computational characteristics of the model and its applicability for the design of an MRI scanner will be illustrated.

2. ACOUSTICS OF FINITE CYLINDRICAL DUCTS WITH PLANAR BAFFLES

The acoustic model for a finite duct with vibrating walls and infinite flanges will be derived in this section. First, the general (infinite) duct acoustic theory that is described in many textbooks (e.g., references [6–8]) will be reviewed briefly. Then, step by step new features are introduced into the model, eventually leading to the desired model. First, a model will be derived that describes the acoustic response of the duct system due to a monopole source inside the duct wall. Then, it will be shown that the description of the acoustic field caused by the vibrating wall of the duct is a generalization of the monopole source model. At the end, the duct acoustics model incorporating wall vibration is coupled with a model for the reflection conditions for the baffle at the finite duct's exits. This results in a general model for the acoustics of finite cylindrical ducts with planar baffles and vibrating walls.

2.1. ACOUSTIC EQUATIONS FOR CYLINDRICAL DUCTS

Consider the sound field in an infinite cylindrical duct with radius $r = a$ with uniform sound speed c_0 and density ρ_0 in the acoustic medium. If only harmonic solutions for the sound field are considered, the acoustic pressure and velocity in the duct can be expressed as

$$\tilde{p}(r, \theta, z, t) = \mathrm{Re}\,[p(r, \theta, z, \omega)\,\mathrm{e}^{\mathrm{i}\omega t}], \qquad \tilde{\mathbf{u}}(r, \theta, z, t) = \mathrm{Re}\,[\mathbf{u}(r, \theta, z, \omega)\,\mathrm{e}^{\mathrm{i}\omega t}], \quad (1)$$

with circular frequency ω. This pressure field has to satisfy the Helmholtz, continuity, state and momentum equations, and is subject to a normal velocity boundary condition at the duct wall:

$$\nabla^2 p + k^2 p = 0, \qquad \mathrm{i}\omega\rho + \rho_0 \nabla \cdot \mathbf{u} = 0, \quad (2, 3)$$

$$p = \rho c_0^2, \qquad \mathrm{i}\rho_0 \omega \mathbf{u} + \nabla p = 0, \qquad u_r|_{\mathrm{wall}} = -\eta(\theta, z), \quad (4\text{–}6)$$

with free field wavenumber $k = \omega/c_0$, u_r the radial component of $\mathbf{u}$, η the given duct wall velocity, and in cylindrical co-ordinates

$$\nabla = \mathbf{e}_r \frac{\partial}{\partial r} + \mathbf{e}_\theta \frac{1}{r}\frac{\partial}{\partial \theta} + \mathbf{e}_z \frac{\partial}{\partial z}, \qquad \nabla^2 = \frac{\partial^2}{\partial r^2} + \frac{1}{r}\frac{\partial}{\partial r} + \frac{1}{r^2}\frac{\partial^2}{\partial \theta^2} + \frac{\partial^2}{\partial z^2}.$$

2.2. THE ACOUSTIC FIELD INSIDE AN INFINITE DUCT

When the sound field in a rigid infinite duct ($\eta = 0$) is considered, the technique of separation of variables can be used to try a solution of the kind $p = f(r)g(\theta)h(z)$. This solution exists if

$$\frac{\partial^2 f}{\partial r^2} + \frac{1}{r}\frac{\partial f}{\partial r} + \left(\alpha^2 - \frac{m^2}{r^2}\right) f = 0, \quad (7a)$$

$$\frac{\partial^2 g}{\partial \theta^2} + m^2 g = 0, \qquad \frac{\partial^2 h}{\partial z^2} + (k^2 - \alpha^2) h = 0, \quad (7b, c)$$

so that $f(r) = \mathrm{J}_m(\alpha_{m\mu} r)$, $\mu = 1, 2, \ldots$, where J_m denotes the ordinary Bessel function of the first kind and $\alpha_{m\mu} = j'_{m\mu}/a$ the radial wavenumber where $j'_{m\mu}$ is the

μth nonnegative non-trivial zero of J'_m, to satisfy the boundary condition $f'|_{r=a} = 0$. The Bessel function of the second kind Y_m is also a solution of equation (7a), but does not satisfy the condition at $r = 0$ where the pressure and its derivative should be finite. Also $g(\theta) = e^{-im\theta}$, $m = \cdots, -2, -1, 0, 1, 2, \ldots$, where use is made of the condition of continuity from $\theta = 2\pi$ to $\theta = 0$. Finally, $h(z) = e^{\mp k_{m\mu} z}$, where $k_{m\mu} = \sqrt{k^2 - \alpha_{m\mu}^2}$ is the axial wavenumber, the square root being defined such that $\mathrm{Re}\,(k_{m\mu}) \geqslant 0$ and $\mathrm{Im}\,(k_{m\mu}) \leqslant 0$. When at a certain free field wavenumber k, the axial wavenumber $k_{m\mu}$ is real, the function $h(z)$ is an oscillatory function, and the corresponding acoustic wave is called cut-on. If $k_{m\mu}$ is imaginary, the function $h(z)$ is exponential and the associated wave is called cut-off.

The *modes*

$$p^{\pm}_{m\mu}(r, \theta, z) = J_m(\alpha_{m\mu} r)\, e^{-im\theta \mp ik_{m\mu} z} \tag{8}$$

form a complete basis [21] for the acoustic field in the duct (with the $+$ and $-$ superscript denoting a wave travelling in the positive or negative z-direction, respectively). Any field in the duct can thus be written by the principle of superposition as the modal expansion

$$p(r, \theta, z) = \sum_{m=-\infty}^{\infty} \sum_{\mu=1}^{\infty} J_m(\alpha_{m\mu} r)\, e^{-im\theta} (A_{m\mu}\, e^{-ik_{m\mu} z} + B_{m\mu}\, e^{ik_{m\mu} z}). \tag{9}$$

This modal expansion is the basis for general duct acoustics (see, e.g., references [6–8]). The plane wave is a special form of this general case with the $m = 0$, $\mu = 1$ mode only.

2.3. RADIATION FROM A POINT SOURCE IN THE WALL OF AN INFINITE DUCT

Consider the field generated inside a rigid walled duct by a volume point source with strength Q at location $r = r_s$, $\theta = \theta_s$, $z = z_s$ defined by

$$i\omega\rho + \rho_0 \nabla \cdot \mathbf{u} = \rho_0 Q \delta(\mathbf{x} - \mathbf{x}_s), \tag{10}$$

inside the duct (see Figure 2). The source strength distribution is given by

$$Q\delta(\mathbf{x} - \mathbf{x}_s) = Q\delta(r - r_s)\delta(z - z_s)\frac{1}{r_s} \sum_{m=-\infty}^{\infty} \delta(\theta - 2\pi m - \theta_s). \tag{11}$$

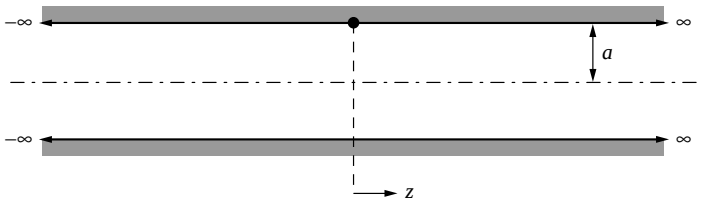

Figure 2. Acoustic source (●) at the wall of an infinite duct.

From causality arguments the generated field should radiate away from the source. A Fourier transformation technique will now be applied to obtain a solution for the acoustic pressure and velocity field that are generated by the point source. A source located on the duct wall $r_s = a$, $\theta_s = 0$, $z_s = 0$, can be represented by the (generalized Fourier transformed) boundary condition (6) at the duct wall:

$$u_r|_{r=a} = \frac{1}{-\mathrm{i}\omega\rho_0}\frac{\partial p}{\partial r}\bigg|_{r=a} = \frac{-Q}{a}\,\delta(z)\sum_{m=-\infty}^{\infty}\delta(\theta - 2\pi m)$$

$$= \frac{-Q}{a}\frac{1}{2\pi}\int_{-\infty}^{\infty}\mathrm{e}^{-\mathrm{i}\gamma z}\,\mathrm{d}\gamma\,\frac{1}{2\pi}\sum_{m=-\infty}^{\infty}\mathrm{e}^{-\mathrm{i}m\theta}. \tag{12}$$

The solution of the wave equation (2) can be found by Fourier transformation in z and Fourier series expansion in θ of the pressure:

$$p(r, \theta, z) = \int_{-\infty}^{\infty}\sum_{m=-\infty}^{\infty}\hat{p}_m(r, \gamma)\,\mathrm{e}^{-\mathrm{i}m\theta - \mathrm{i}\gamma z}\,\mathrm{d}\gamma, \tag{13}$$

$$\hat{p}_m(r, \gamma) = A_m(\gamma)\mathrm{J}_m(\alpha(\gamma)r), \qquad \alpha(\gamma)^2 = k^2 - \gamma^2. \tag{14, 15}$$

From the boundary condition (6) at $r = a$ it follows that

$$\alpha A_m \mathrm{J}'_m(\alpha a) = -\omega\rho_0 Q/a4\pi^2\mathrm{i}, \tag{16}$$

$$p(r, \theta, z) = \frac{-k\rho_0 c_0 Q}{4\pi^2\mathrm{i}}\sum_{m=-\infty}^{\infty}\mathrm{e}^{-\mathrm{i}m\theta}\int_{-\infty}^{\infty}\frac{\mathrm{J}_m(\alpha r)}{\alpha a\mathrm{J}'_m(\alpha a)}\,\mathrm{e}^{-\mathrm{i}\gamma z}\,\mathrm{d}\gamma. \tag{17}$$

The residue integration method (see, e.g., reference [22], chapter 15), is applied to compute the integral equation (17). To satisfy causality, the integration contour is indented above the poles $\gamma = k_{m\mu}$ and below the poles $\gamma = -k_{m\mu}$, and the contour closed through the lower half plane for positive z and through the negative half plane for negative z (see e.g., references [6, p. 17; 7, p. 652]). The solution can be written as

$$p(r, \theta, z) = \frac{\rho_0 c_0}{2\pi}\sum_{m=-\infty}^{\infty}\mathrm{e}^{-\mathrm{i}m\theta}\sum_{\mu=1}^{\infty}\frac{\alpha_{m\mu}^2 a^2}{\alpha_{m\mu}^2 a^2 - m^2}\frac{\mathrm{J}_m(\alpha_{m\mu}r)}{\mathrm{J}_m(\alpha_{m\mu}a)}\frac{kQ}{k_{m\mu}a^2}\,\mathrm{e}^{-\mathrm{i}k_{m\mu}|z|}, \tag{18}$$

of which the plane wave component is

$$p(r, \theta, z) = \frac{\rho_0 c_0}{2\pi}\frac{Q}{a^2}\,\mathrm{e}^{-\mathrm{i}k_{m\mu}|z|}.$$

This result is an expression for the acoustic impulse response of the infinite duct valid for any non-resonant frequency ($k_{m\mu} \neq 0$). In the source plane $z = z_s = 0$, the series for p is conditionally convergent. The series for the velocity **u** here is not

convergent at all in the usual sense, but has to be interpreted as a generalized function, as might be expected from the δ-type source.

2.4. RADIATION FROM A FINITE PART OF THE WALL INSIDE A INFINITE DUCT

If a finite part (between $-L \leqslant z \leqslant L$) of the wall (at $r = a$) inside an infinite duct is vibrating and radiating sound (see Figure 3), the velocity at the wall can be described as

$$u_r(a, \theta, z) = -\eta(\theta, z) \quad \text{for} \quad -L \leqslant z \leqslant L. \tag{19}$$

For each frequency ω, the solution of this problem can be found with the Fourier transformation method analogous to the method described for the simple source radiation. Again, from causality, the field should be outward radiating in $|z| > L$. The boundary condition at the duct wall can again be written as a Fourier sum:

$$u_r(r = a, \theta, z) = -\frac{1}{\mathrm{i}\omega\rho_0}\frac{\partial p}{\partial r}\bigg|_{r=a} = -\frac{1}{2\pi}\sum_{m=-\infty}^{\infty} \mathrm{e}^{-\mathrm{i}m\theta}\eta_m(z)$$

$$= -\frac{1}{4\pi^2}\sum_{m=-\infty}^{\infty} \mathrm{e}^{-\mathrm{i}m\theta}\int_{-\infty}^{\infty} \hat{\eta}_m(\gamma)\,\mathrm{e}^{-\mathrm{i}\gamma z}\,\mathrm{d}\gamma, \tag{20}$$

where the Fourier coefficients $\hat{\eta}_m(\gamma)$ of the wall velocity $\eta_m(\theta, z)$ are defined by

$$\hat{\eta}_m(\gamma) = \int_{-\infty}^{\infty} \mathrm{e}^{\mathrm{i}\gamma z}\int_0^{2\pi} \eta(\theta, z)\,\mathrm{e}^{\mathrm{i}m\theta}\,\mathrm{d}\theta\,\mathrm{d}z = \int_{-L}^{L}\int_0^{2\pi} \eta(\theta, z)\,\mathrm{e}^{\mathrm{i}m\theta + \mathrm{i}\gamma z}\,\mathrm{d}\theta\,\mathrm{d}z. \tag{21}$$

For the pressure in the duct, the modal expansion as in equations (13)–(15) can be used,

$$p(r, \theta, z) = \int_{-\infty}^{\infty}\sum_{m=-\infty}^{\infty} \hat{p}_m(r, \gamma)\,\mathrm{e}^{-\mathrm{i}m\theta - \mathrm{i}\gamma z}\,\mathrm{d}\gamma,$$

with

$$\hat{p}_m(r, \gamma) = A_m(\gamma)\mathrm{J}_m(\alpha(\gamma)r), \qquad \alpha(\gamma)^2 = k^2 - \gamma^2.$$

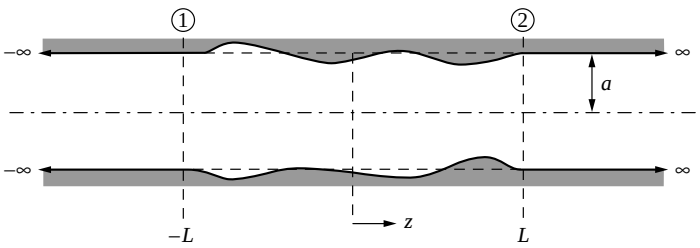

Figure 3. Vibrating walls inside an infinite duct.

Substituting this expansion in equation (20) for the boundary condition at the duct wall results in

$$\alpha A_m \mathrm{J}'_m(\alpha a) = -\frac{\rho_0 \omega}{4\pi^2 \mathrm{i}} \hat{\eta}_m, \tag{22}$$

$$p(r, \theta, z) = -\frac{k\rho_0 c_0 a}{4\pi^2 \mathrm{i}} \sum_{m=-\infty}^{\infty} \mathrm{e}^{-\mathrm{i}m\theta} \int_{-\infty}^{\infty} \frac{\mathrm{J}_m(\alpha r)}{\alpha a \mathrm{J}'_m(\alpha a)} \hat{\eta}_m(\gamma)\, \mathrm{e}^{-\mathrm{i}\gamma z}\, \mathrm{d}\gamma$$

$$= -\frac{k\rho_0 c_0 a}{4\pi^2 \mathrm{i}} \sum_{m=-\infty}^{\infty} \mathrm{e}^{-\mathrm{i}m\theta} \int_{-L}^{L} \int_{-\infty}^{\infty} \frac{\mathrm{J}_m(\alpha r)}{\alpha a \mathrm{J}'_m(\alpha a)} \mathrm{e}^{-\mathrm{i}\gamma(z-z')}\, \mathrm{d}\gamma\, \eta_m(z')\, \mathrm{d}z'. \tag{23}$$

Similar to the "source in the hard walled duct" case, the integral in this equation can be computed with the residue integration method since $\hat{\eta}_m(\gamma)$ is analytic everywhere because it is defined as a finite integral. This results in

$$p(r, \theta, z) = \frac{\rho_0 c_0}{2\pi} \sum_{m=-\infty}^{\infty} \mathrm{e}^{-\mathrm{i}m\theta} \sum_{\mu=1}^{\infty} \frac{\alpha_{m\mu}^2 a^2}{\alpha_{m\mu}^2 a^2 - m^2} \frac{\mathrm{J}_m(\alpha_{m\mu} r)}{\mathrm{J}_m(\alpha_{m\mu} a)} \times \frac{k}{k_{m\mu} a} \int_{-L}^{L} \eta_m(z')\, \mathrm{e}^{-\mathrm{i}k_{m\mu}|z-z'|}\, \mathrm{d}z', \tag{24}$$

valid for any non-resonance frequency ($k_{m\mu} \neq 0$). This result denotes the convolution of the acoustic impulse response [equation (18)], and the circumferential Fourier coefficients of the wall velocity $\eta_m(z)$. A bit confusing may be the observation that the resulting series for the velocity u_r appears to be a sum of hard-wall modes. Since every term in the velocity series vanishes at the wall, it might *seem* that the series also vanishes at the wall, in contrast to the boundary condition! This is, however, only pointwise, because the series does not converge uniformly near $r = a$ (see e.g., reference [22], chapter 14). In any neighborhood of $r = a$ the series behaves according to the boundary condition. Furthermore, an order of magnitude estimate of the terms of the series shows that the series for p converges absolutely, and for u_r converges conditionally.

2.5. RADIATION FROM A FINITE DUCT TERMINATING IN INFINITE FLANGES

The radiation from the walls of a finite duct terminating in rigid baffles (see Figure 4) is considerably more complex than the former three situations. This is caused by the "interface" impedances at the duct's exits. An acoustic wave that is incident to the plane of termination of the duct in a rigid baffle is partly transmitted and partly reflected. The reflection is rather complex because there generally is coupling between the radial modes of the incident and reflected acoustic field. Zorumski [12] has described a method to compute the generalized radiation impedances and reflection coefficients of circular ducts. This is needed to impose the boundary conditions for the sound radiation model for baffled finite ducts. It will be shown that the model for the radiation of a vibrating wall in an infinite duct can be combined with the reflection coefficients to impose the boundary conditions at the duct's exits.

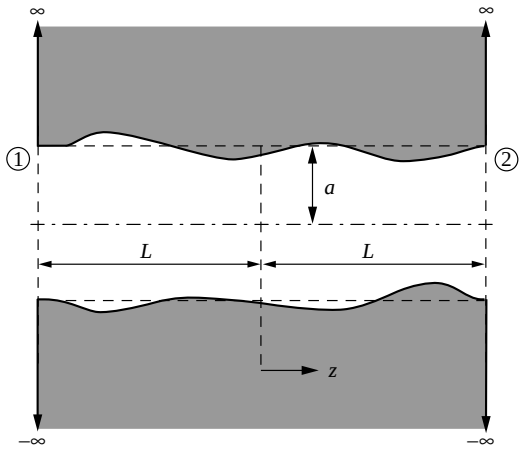

Figure 4. Vibrating walls inside a baffled finite duct.

2.5.1. *Generalized radiation impedances*

Consider the radiation of sound from a circular duct terminating in a planar baffle (infinite flange). The pressure and axial velocity at the duct exit (with $z = z_e = \pm L$, as in Figure 4) can be written as a complete sum of eigenmodes in radial r and circumferential θ direction is (equation (9)),

$$p(r, \theta, z_e) = \sum_{m=-\infty}^{\infty} \mathrm{e}^{-\mathrm{i}m\theta} \sum_{\mu=1}^{\infty} P_{m\mu} \mathrm{J}_m(\alpha_{m\mu} r), \tag{25}$$

$$u_z(r, \theta, z_e) = \frac{1}{\rho_0 c_0} \sum_{m=-\infty}^{\infty} \mathrm{e}^{-\mathrm{i}m\theta} \sum_{\mu=1}^{\infty} V_{m\mu} \mathrm{J}_m(\alpha_{m\mu} r), \tag{26}$$

with modal coefficients $P_{m\mu}$ and $V_{m\mu}$ for the pressure and velocity, respectively. Zorumski [12] has shown that these coefficients are coupled by so-called generalized radiation impedances (see Appendix A)

$$P_{m\mu} = \sum_{\nu=1}^{\infty} Z_{m\mu\nu} V_{m\nu}, \tag{27}$$

where μ is the radial order of the incident mode, ν is the radial order of the reflected mode, and

$$Z_{m\mu\nu} = \frac{1}{N_{m\mu}^2} \int_0^{\infty} \frac{\tau}{\sqrt{1-\tau^2}} D_{m\mu}(\tau) D_{m\nu}(\tau)\, \mathrm{d}\tau, \tag{28}$$

$$N_{m\mu}^2 = \tfrac{1}{2}(a^2 - m^2/\alpha_{m\mu}^2)\mathrm{J}_m(\alpha_{m\mu} a)^2, \tag{29}$$

$$D_{m\mu}(\tau) = \frac{\tau k^2 a}{\alpha_{m\mu}^2 - \tau^2 k^2} \mathrm{J}'_m(\tau k a)\mathrm{J}_m(\alpha_{m\mu} a). \tag{30}$$

Equation (27) shows that energy from a single incident radial mode is transferred into all reflected (and transmitted) radial modes. Because of the oscillatory nature of the integrand in equation (28) the evaluation of this integral is not straightforward. This is discussed in Appendix B.

2.5.2. *Accounting for planar baffles in a finite duct*

The problem of a vibrating duct wall that radiates sound into a finite duct terminating in planar baffles is an extension of the problem of a vibrating wall in an infinite duct. The baffle interface acts as an additional generalized impedance in the duct, where incident waves are partly transmitted and partly reflected. The total solution for the pressure has to satisfy both the boundary conditions at the duct wall and at the interface at the duct's exits. Since the boundary conditions at the wall are similar for the finite and infinite duct problems it is convenient to use this solution (denoted as p') and adding to this solution a homogeneous solution, i.e., a general duct acoustic pressure field p'' with vanishing velocity at the wall. This is possible because the equations are linear.

The pressure in the finite duct can be written as

$$p(r, \theta, z) = p'(r, \theta, z) + p''(r, \theta, z), \tag{31}$$

with

$$p'(r, \theta, z) = \frac{\rho_0 c_0}{2\pi} \sum_{m=-\infty}^{\infty} \mathrm{e}^{-\mathrm{i}m\theta} \sum_{\mu=1}^{\infty} \frac{\alpha_{m\mu}^2 a^2}{\alpha_{m\mu}^2 a^2 - m^2} \frac{\mathrm{J}_m(\alpha_{m\mu} r)}{\mathrm{J}_m(\alpha_{m\mu} a)}$$

$$\times \frac{k}{k_{m\mu} a} \int_{-L}^{L} \eta_m(z') \, \mathrm{e}^{-\mathrm{i}k_{m\mu}|z - z'|} \, \mathrm{d}z', \tag{32}$$

$$p''(r, \theta, z) = \sum_{m=-\infty}^{\infty} \sum_{\mu=1}^{\infty} \mathrm{J}_m(\alpha_{m\mu} r) \, \mathrm{e}^{-\mathrm{i}m\theta} (A''_{m\mu} \, \mathrm{e}^{-\mathrm{i}k_{m\mu} z} + B''_{m\mu} \, \mathrm{e}^{\mathrm{i}k_{m\mu} z}), \tag{33}$$

where $(\alpha_{m\mu}^2 a^2)/(\alpha_{m\mu}^2 a^2 - m^2) = 1$ if $m = 0$, $\mu = 1$. The total pressure p has to satisfy the boundary condition

$$\left. \frac{\partial p}{\partial r} \right|_{r=a} = \frac{\partial}{\partial r} (p' + p'')|_{r=a} = -\mathrm{i}\omega \rho_0 u_r(r = a, \theta, z). \tag{34}$$

The pressure field p' already satisfies this boundary condition as defined in equation (20), thus, for p'' the following boundary condition must hold:

$$\left. \frac{\partial p''}{\partial r} \right|_{r=a} = 0. \tag{35}$$

Since every term in the series of p'' satisfies this condition, it will be satisfied by the infinite sum if the series converges uniformly (for example if the series consists of a finite number of terms). This is a rather subtle point because p' is a series of the same form as p'', but $\partial p'/\partial r$ does *not* converge uniformly. Therefore, the

uniform convergence condition for p'' is essential for the split-up of p, but appears to be satisfied in practice. Hence, the sound field that is generated in the finite duct is a superposition of the sound field generated by the vibrating walls in an infinite duct and the homogeneous sound field satisfying the velocity boundary condition $u_r = 0$ at $r = a$. The modal coefficients $A''_{m\mu}$ and $B''_{m\mu}$ will be determined by the condition that the total solution has to satisfy the reflection boundary conditions at the duct's exits ($z = \pm L$). The total acoustic pressure can thus be written as

$$p(r, \theta, z) = \sum_{m=-\infty}^{\infty} \sum_{\mu=1}^{\infty} \mathrm{J}_m(\alpha_{m\mu} r)\, \mathrm{e}^{-\mathrm{i}m\theta}(A_{m\mu}(z)\, \mathrm{e}^{-\mathrm{i}k_{m\mu} z} + B_{m\mu}(z)\, \mathrm{e}^{\mathrm{i}k_{m\mu} z}), \tag{36}$$

with

$$A_{m\mu}(z) = A''_{m\mu} + \frac{\alpha_{m\mu}^2 a^2}{\alpha_{m\mu}^2 a^2 - m^2} \frac{1}{\mathrm{J}_m(\alpha_{m\mu} a)} \frac{\rho_0 c_0 k}{2\pi a k_{m\mu}} \int_{-L}^{z} \eta_m(z')\, \mathrm{e}^{\mathrm{i}k_{m\mu} z'}\, \mathrm{d}z', \tag{37a}$$

$$B_{m\mu}(z) = B''_{m\mu} + \frac{\alpha_{m\mu}^2 a^2}{\alpha_{m\mu}^2 a^2 - m^2} \frac{1}{\mathrm{J}_m(\alpha_{m\mu} a)} \frac{\rho_0 c_0 k}{2\pi a k_{m\mu}} \int_{z}^{L} \eta_m(z')\, \mathrm{e}^{-\mathrm{i}k_{m\mu} z'}\, \mathrm{d}z'. \tag{37b}$$

At the interface, the generalized impedances defined in the previous section can be used to obtain a relationship between the modal coefficients of the pressure and velocity at the duct's exits. The value of the pressure, velocity and their modal coefficients at interfaces 1 and 2 in Figure 4 are identified by superscripts 1 and 2. At interface 1, p' can be written as

$$p'(r, \theta, z = -L) = p'^1 = \sum_{m=-\infty}^{\infty} \sum_{\mu=1}^{\infty} \mathrm{J}_m(\alpha_{m\mu} r)\, \mathrm{e}^{-\mathrm{i}m\theta}(H^1_{m\mu}\, \mathrm{e}^{-\mathrm{i}k_{m\mu} L}), \tag{38}$$

with

$$H^1_{m\mu} = \frac{\alpha_{m\mu}^2 a^2}{\alpha_{m\mu}^2 a^2 - m^2} \frac{1}{\mathrm{J}_m(\alpha_{m\mu} a)} \frac{\rho_0 c_0 k}{2\pi a k_{m\mu}} \int_{-L}^{L} \eta_m(z')\, \mathrm{e}^{-\mathrm{i}k_{m\mu} z'}\, \mathrm{d}z'. \tag{39}$$

Thus, the total pressure p at interface 1 is given by

$$p(r, \theta, z = -L) = p^1 = \sum_{m=-\infty}^{\infty} \sum_{\mu=1}^{\infty} \mathrm{J}_m(\alpha_{m\mu} r)\, \mathrm{e}^{-\mathrm{i}m\theta}(A''_{m\mu}\, \mathrm{e}^{\mathrm{i}k_{m\mu} L} + (H^1_{m\mu} + B''_{m\mu})\, \mathrm{e}^{-\mathrm{i}k_{m\mu} L}). \tag{40}$$

The axial velocity $u_z(r, \theta, z)$ *in the negative z direction* can be written as

$$u_z(r, \theta, z = -L) = u_z^1 = \frac{1}{\mathrm{i}\omega\rho_0} \frac{\partial p}{\partial z}\bigg|_{z=-L}$$

$$= \sum_{m=-\infty}^{\infty} \sum_{\nu=1}^{\infty} \mathrm{J}_m(\alpha_{m\nu} r)\, \mathrm{e}^{-\mathrm{i}m\theta} \frac{k_{m\nu}}{\omega\rho_0} (A''_{m\nu}\, \mathrm{e}^{\mathrm{i}k_{m\nu} L} - (H^1_{m\nu} + B''_{m\nu})\, \mathrm{e}^{-\mathrm{i}k_{m\nu} L}). \tag{41}$$

The coefficients of the pressure and axial velocity at interface 1 from equations (25) and (26), respectively, can be written as

$$P^1_{m\mu} = A''_{m\mu}\, \mathrm{e}^{\mathrm{i}k_{m\mu}L} + (H^1_{m\mu} + B''_{m\mu})\, \mathrm{e}^{-\mathrm{i}k_{m\mu}L}, \tag{42}$$

$$V^1_{mv} = \frac{k_{mv}}{k}\,(-A''_{mv}\, \mathrm{e}^{\mathrm{i}k_{mv}L} + (H^1_{mv} + B''_{mv})\, \mathrm{e}^{-\mathrm{i}k_{mv}L}). \tag{43}$$

These expressions can be sutstituted into equation (27) (which is allowed because the boundary conditions at the duct wall for p' and p'' both satisfy $\mathrm{J}'(\alpha_{m\mu}a) = 0$). This substitution gives

$$A''_{m\mu}\, \mathrm{e}^{\mathrm{i}k_{m\mu}L} + (H^1_{m\mu} + B''_{m\mu})\, \mathrm{e}^{-\mathrm{i}k_{m\mu}L} = \sum_{v=1}^{\infty} Z^1_{m\mu v}\, \frac{k_{mv}}{k}\, [(H^1_{mv} + B''_{mv})\, \mathrm{e}^{-\mathrm{i}k_{mv}L} - A''_{mv}\, \mathrm{e}^{\mathrm{i}k_{mv}L}], \tag{44}$$

or

$$\sum_{v=1}^{\infty} \left(Z^1_{m\mu v}\, \frac{k_{mv}}{k} + \delta_{\mu v} \right) A''_{mv}\, \mathrm{e}^{\mathrm{i}k_{mv}L} = \sum_{v=1}^{\infty} \left(Z^1_{m\mu v}\, \frac{k_{mv}}{k} - \delta_{\mu v} \right) (H^1_{mv} + B''_{mv})\, \mathrm{e}^{-\mathrm{i}k_{mv}L}. \tag{45}$$

Upon introducing the variable

$$E_{mv}(z) = \mathrm{e}^{-\mathrm{i}k_{\mu v}z}, \tag{46}$$

equation (45) can be written as

$$E_{mv}(-L)A''_{mv} = \sum_{v=1}^{\infty} R^1_{m\mu v} E_{m\mu}(L)(B''_{m\mu} + H^1_{mv}), \quad \text{for} \quad \begin{cases} m = 0, \pm 1, \pm 2, \ldots \\ \mu = 1, 2, 3, \ldots \end{cases}. \tag{47}$$

The terms $R^1_{m\mu v}$ are the reflection coefficients that can be related to the modal impedance $Z^1_{m\mu v}$ by the following *infinite* matrix equation. For a given azimuthal order m, the reflection coefficient $R^1_{m\mu v}$ is element (μ, v) of reflection matrix $\mathbf{R}^1_m$ at interface 1:

$$\mathbf{R}^1_m = [\mathbf{Z}^1_m \mathbf{K}_m + \mathbf{I}]^{-1} [\mathbf{Z}^1_m \mathbf{K}_m - \mathbf{I}], \tag{48}$$

where $\mathbf{I}$ is the identity matrix, and $\mathbf{K}_m$ is a diagonal matrix which is, for *fixed* azimuthal order m, given by

$$\mathbf{K}_m = \begin{bmatrix} k_{m1}/k & 0 & \cdots & 0 & \cdots \\ 0 & k_{m2}/k & \cdots & 0 & \cdots \\ \vdots & \vdots & \ddots & \vdots & \vdots \\ 0 & 0 & \cdots & k_{mv}/k & \cdots \\ \vdots & \vdots & \cdots & \vdots & \ddots \end{bmatrix}. \tag{49}$$

Because m is fixed, $\mathbf{K}$ is only valid for *one value* of the azimuthal order at a time, and generally will be different for each value of m. Here v is the radial order of the reflected modes, where $1 \leqslant v \leqslant \infty$. The (generally non-symmetric) matrix of reflection coefficients is defined as

$$\mathbf{R}_m^1 = \begin{bmatrix} R_{m11}^1 & R_{m12}^1 & \cdots & R_{m1v}^1 & \cdots \\ R_{m21}^1 & R_{m22}^1 & \cdots & R_{m2v}^1 & \cdots \\ \vdots & \vdots & \ddots & \vdots & \vdots \\ R_{m\mu1}^1 & R_{m\mu2}^1 & \cdots & R_{m\mu v}^1 & \cdots \\ \vdots & \vdots & \cdots & \vdots & \ddots \end{bmatrix}, \tag{50}$$

where the impedance matrix is given by

$$\mathbf{Z}_m^1 = \begin{bmatrix} Z_{m11}^1 & Z_{m12}^1 & \cdots & Z_{m1v}^1 & \cdots \\ Z_{m21}^1 & Z_{m22}^1 & \cdots & Z_{m2v}^1 & \cdots \\ \vdots & \vdots & \ddots & \vdots & \vdots \\ Z_{m\mu1}^1 & Z_{m\mu2}^1 & \cdots & Z_{m\mu v}^1 & \cdots \\ \vdots & \vdots & \cdots & \vdots & \ddots \end{bmatrix}. \tag{51}$$

Expression (47) for the reflection at interface 1 can be written as a matrix equation,

$$\mathbf{E}_m(-L)\mathbf{a}_m = \mathbf{R}_m^1 \mathbf{E}_m(L)(\mathbf{b}_m + \mathbf{h}_m^1), \tag{52}$$

with

$$\mathbf{E}_m(z) = \begin{bmatrix} \mathrm{e}^{-\mathrm{i}k_{m1}z} & 0 & \cdots & 0 & \cdots \\ 0 & \mathrm{e}^{-\mathrm{i}k_{m2}z} & \cdots & 0 & \cdots \\ \vdots & \vdots & \ddots & \vdots & \vdots \\ 0 & 0 & \cdots & \mathrm{e}^{-\mathrm{i}k_{mv}z} & \cdots \\ \vdots & \vdots & \cdots & \vdots & \ddots \end{bmatrix}, \tag{53}$$

and

$$\mathbf{a}_m = [A_{m1}'' \quad A_{m2}'' \quad \cdots \quad A_{mv}'' \quad \cdots]^{\mathrm{T}}, \tag{54}$$

$$\mathbf{b}_m = [B_{m1}'' \quad B_{m2}'' \quad \cdots \quad B_{mv}'' \quad \cdots]^{\mathrm{T}}, \tag{55}$$

$$\mathbf{h}_m^1 = [H_{m1}^1 \quad H_{m2}^1 \quad \cdots \quad H_{mv}^1 \quad \cdots]^{\mathrm{T}}. \tag{56}$$

Similarly, at interface 2 the matrix equation

$$\mathbf{E}_m(-L)\mathbf{b}_m = \mathbf{R}_m^2 \mathbf{E}_m(L)(\mathbf{a}_m + \mathbf{h}_m^2), \tag{57}$$

can be derived, with

$$\mathbf{R}_m^2 = [\mathbf{Z}_m^2 \mathbf{K}_m + \mathbf{I}]^{-1}[\mathbf{Z}_m^2 \mathbf{K}_m - \mathbf{I}]. \tag{58}$$

3. NUMERICAL IMPLEMENTATION

The matrices in equations (52) and (57) are infinite in size and can therefore not be readily manipulated numerically. In general the infinite matrices are truncated to a maximum $v = N$, and a set of $2N$ equations with $2N$ unknowns (the elements of $\mathbf{a}_m$ and $\mathbf{b}_m$) is obtained for every azimuthal order m. When this system is solved an explicit (approximate) expression for p'' is obtained and this leads to a closed form solution for the total pressure,

$$p(r, \theta, z) = \sum_{m=-\infty}^{\infty} \sum_{\mu=1}^{N} \mathrm{J}_m(\alpha_{m\mu} r)\, \mathrm{e}^{-\mathrm{i}m\theta}(A_{m\mu}(z)\, \mathrm{e}^{-\mathrm{i}k_{m\mu}z} + B_{m\mu}(z)\, \mathrm{e}^{\mathrm{i}k_{m\mu}z}), \tag{59}$$

with amplitudes $A_{m\mu}(z)$ and $B_{m\mu}(z)$ as in equation (37). After truncation there remain two problems to be solved: calculation of the integrals in equation (37); solving the coupled truncated matrix equations (52) and (57). The implementation details of a solution of these problems will be presented next.

3.1. FOURIER INTEGRAL CALCULATION

In order to use the proposed formulation for the pressure in a finite (planar) baffled duct, the convolution between the Fourier coefficients (with respect to the circumferential direction) of the wall velocity $\eta_m(z)$ and the function $\mathrm{e}^{-\mathrm{i}k_{m\mu}|z|}$ needs to be computed:

$$I = \int_{-L}^{L} \eta_m(z')\, \mathrm{e}^{-\mathrm{i}k_{m\mu}|z - z'|}\, \mathrm{d}z'. \tag{60}$$

This integral has to be computed for every circumferential mode m and every radial mode μ. The integral can be split into the ranges $[-L, z]$ and $[z, L]$. Then the absolute value operator in the exponential function can be removed:

$$I = \int_{-L}^{z} \eta_m(z')\, \mathrm{e}^{-\mathrm{i}k_{m\mu}(z - z')}\, \mathrm{d}z' + \int_{z}^{L} \eta_m(z')\, \mathrm{e}^{-\mathrm{i}k_{m\mu}(z' - z)}\, \mathrm{d}z'. \tag{61}$$

Since both integrals are bounded for all z, numerical integration is rather straightforward. When $k_{m\mu}$ is real, the duct wall normal velocity is multiplied with an oscillating function yielding a oscillating integrand. Therefore, the trapezoidal rule or Romberg integration should be used because these methods have a better convergence than Gauss-Legendre integration for oscillating integrands. When $k_{m\mu}$ is imaginary (and thus negative), the normal velocity is multiplied with an exponentially decaying function, yielding an exponentially decaying integrand. This type of integrand can also be integrated efficiently with the trapezoidal rule or Romberg integration.

3.2. MATRIX EQUATION SOLUTION

After truncation of matrix equations (52) and (57), the coupled matrix equations

$$\mathbf{R}^1\mathbf{E}(L)(\mathbf{a} + \mathbf{h}^1) = \mathbf{E}(-L)\mathbf{b}, \qquad \mathbf{R}^2\mathbf{E}(L)(\mathbf{b} + \mathbf{h}^2) = \mathbf{E}(-L)\mathbf{a}, \tag{62a, b}$$

(where subscript m has been suppressed for clarity) need to be solved simultaneously to obtain values for the amplitudes $A''_{m\mu}$ and $B''_{m\mu}$, which are the elements of vectors **a** and **b**, respectively. The main problem in obtaining this solution are the low condition numbers of matrices $\mathbf{R}^1$, $\mathbf{R}^2$ and $\mathbf{E}(\pm L)$, so the solution of the system is not straightforward.

Since both ends of the duct are simlar (but mirrored), the reflection behavior of the sound waves is also similar. Therefore the reflection matrices at both ends are the same: $\mathbf{R}^1 = \mathbf{R}^2 = \mathbf{R}$. Equations (62a) and (62b) are then added up and $\mathbf{r}_+ = \mathbf{a} + \mathbf{b}$ is introduced, to obtain

$$[\mathbf{I} - \mathbf{E}(L)\mathbf{R}\mathbf{E}(L)]\mathbf{r}_+ = \mathbf{E}(L)\mathbf{R}\mathbf{E}(L)[\mathbf{h}^2 + \mathbf{h}^1]. \tag{63a}$$

Equation (62b) subtracted from equation (62a) and introducing $\mathbf{r}_- = \mathbf{a} - \mathbf{b}$ yields

$$[\mathbf{I} + \mathbf{E}(L)\mathbf{R}\mathbf{E}(L)]\mathbf{r}_- = \mathbf{E}(L)\mathbf{R}\mathbf{E}(L)[\mathbf{h}^2 - \mathbf{h}^1]. \tag{63b}$$

Both equations can now be solved separately for $\mathbf{r}_+$ and $\mathbf{r}_-$. The vectors **a** and **b** are simply related to these vectors:

$$\mathbf{a} = \tfrac{1}{2}(\mathbf{r}_+ + \mathbf{r}_-), \qquad \mathbf{b} = \tfrac{1}{2}(\mathbf{r}_+ - \mathbf{r}_-). \tag{64a, b}$$

Using this solution strategy is advantageous over direct substitution of equation (62b) in equation (62a), because in that case the matrix product $\mathbf{E}(L)^2$ is introduced which leads to numerical underflow errors for large values of L.

The coupled matrix equations (62) can also be solved iteratively by using the recurrent relationship

$$\mathbf{a}_{i+1} = \mathbf{E}(L)\mathbf{R}\mathbf{E}(L)[\mathbf{b}_i + \mathbf{h}^1], \qquad \mathbf{b}_{i+1} = \mathbf{E}(L)\mathbf{R}\mathbf{E}(L)[\mathbf{a}_i + \mathbf{h}^2], \tag{65a, b}$$

and starting the recursion with $\mathbf{a}_0 = \mathbf{0}$, $\mathbf{b}_0 = \mathbf{0}$. A good measure for the convergence of the iteration is the relative difference in the acoustic power radiated out of the baffled duct between two subsequent iterations (see Appendix C for the power relations).

4. NUMERICAL EXPERIMENTS AND RESULTS

To explore the characteristics of the presented baffled duct (BD) model, a number of numerical experiments were performed. The model was compared with an analogous configuration implemented in an acoustic Fourier Boundary Element Method (FBEM) model with the program bArd [23]. This was done to investigate its applicability for modelling the acoustic response of an MRI-scanner. Secondly, the "internal" characteristics of the BD model were investigated with a parameter study, in which the truncation of the Fourier–Bessel series [equation (59)] was varied.

4.1. COMPARISON WITH FOURIER BEM MODELS

The baffled duct model that was used in the numerical experiments consists of a duct with half length $L = 1$ m and radius $a = 0{\cdot}5$ m. The Fourier BEM model that was used for comparison can be viewed as a thick walled version of a duct with the same length and radius as the baffled duct model. In three distinct versions

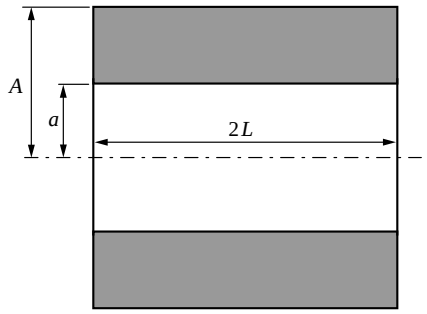

Figure 5. Duct model for FBEM calculations.

of the BEM model the duct's outer radius was taken as $A = 0{\cdot}75$ m, $A = 1{\cdot}0$ m, and $A = 5{\cdot}0$ m, respectively (see Figure 5).

To assess the applicability of the baffled duct model as an alternative to the FBEM model, the acoustic response of the BD model was computed at 23 frequencies in the range 90–1100 Hz. The velocity boundary condition at the wall inside the duct was defined as a half sine function for all frequencies,

$$u_r(a, \theta, z) = u_a \cos(z\pi/2L) \cos(m\theta),$$

with $u_a = 10^{-4}$ m/s arbitrarily chosen. Three circumferential harmonic numbers $m = 0, 1, 2$ were used in the calculations. The infinite Fourier–Bessel series in the baffled duct formulation was truncated at $N = 30$ terms. The acoustic responses of the three FBEM models with varying thicknesses, subjected to the same boundary conditions inside the duct, were also computed. The outer wall of the duct was modelled as rigid. For all models, the values for speed of sound and density of the air were taken as $c = 343$ m/s, and $\rho = 1{\cdot}21$ kg/m^3.

The BD and FBEM models are compared for both radiated acoustic power and average acoustic wall pressure amplitude. The radiated power is a measure for the farfield response, while the average amplitude of the wall pressure is a measure for the near field response of the models. The results for these quantities for harmonics 0, 1 and 2 are shown in Figures 6, 7 and 8. The pressure difference is defined as the difference between average pressure amplitude of the FBEM model and the BD model ($A = \infty$) and is also shown in Figures 6, 7 and 8.

The radiated power spectra of the FBEM models closely resemble the spectrum for the BD model. The spectra deviate only for relatively low frequencies. As could have been anticipated, the upper limit of the low frequency range is the frequency where the acoustic wavelength ($\lambda = c/f$) is of the same order as the outer radius of the duct in the BEM model. Above this frequency (450, 340 and 70 Hz for respectively $A = 0{\cdot}75$, 1 and 5 m), the acoustic field in the duct "sees" the duct as having infinite flanges.

The average wall pressure amplitude results for the FBEM duct models correspond very well to the results of the BD duct model. The correspondence is even better than the resemblance for the power results, especially in the low frequency range. This means that the near field in the duct is rather insensitive to the boundary conditions at the outside of the duct. The pressure difference results

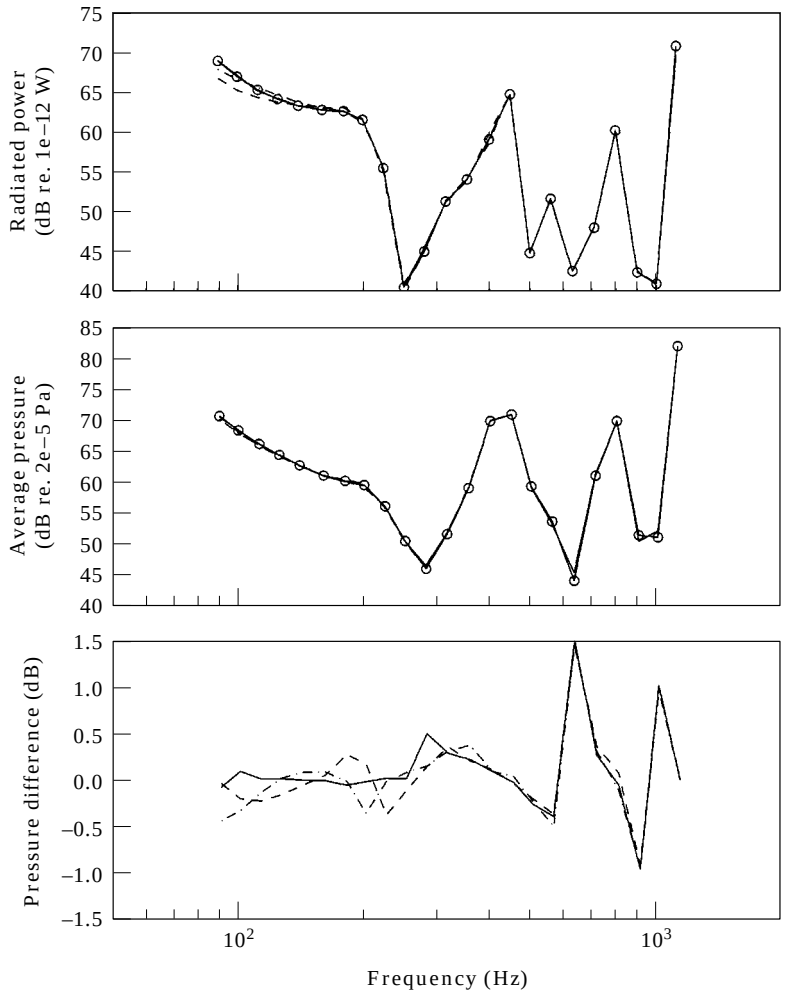

Figure 6. Acoustic responses for circumferential harmonic $m = 0$ for different outer radii. Half-sine excitation. A values: ——, 0·75; · – · – · , 1·0; ——, 5·0; ○——○, ∞.

show that the maximum difference in near field pressure is at most approximately 1 dB. Furthermore, it is noticed that the pressure differences manifest themselves mainly for low average pressure amplitute values, which are of lesser importance in the MRI design process. In the high frequency region, the pressure differences between the three BEM models and the BD model evince identical behavior, so it is expected that these pressure differences can be attributed to the intrinsic differences between FBEM and BD models, rather than to the geometric differences.

It can be concluded that the BD model is a sufficiently accurate approximation for a thick-walled duct with inner wall vibration with an outer radius larger than $A = 0{\cdot}75$ m.

4.2. CHARACTERISTICS OF THE BAFFLED DUCT MODEL

The influence of the truncation of the Fourier–Bessel series in equation (59) on the response of the baffled duct model was assessed. To that end, the number of terms in the series N was varied: $N = 5$, 10, 30 and 50. As a reference, these results were compared with the results of the FBEM model with outer radius $A = 5{\cdot}0$ m. The acoustic response computed with these parameters is depicted in Figures 9, 10 and 11. The pressure difference is now defined as the difference between the average wall pressure amplitude of the BD model and the average wall pressure amplitude of the FBEM model.

The results for the radiated acoustic power as a function of the frequency indicate that a good approximation can be made with only five modes in the

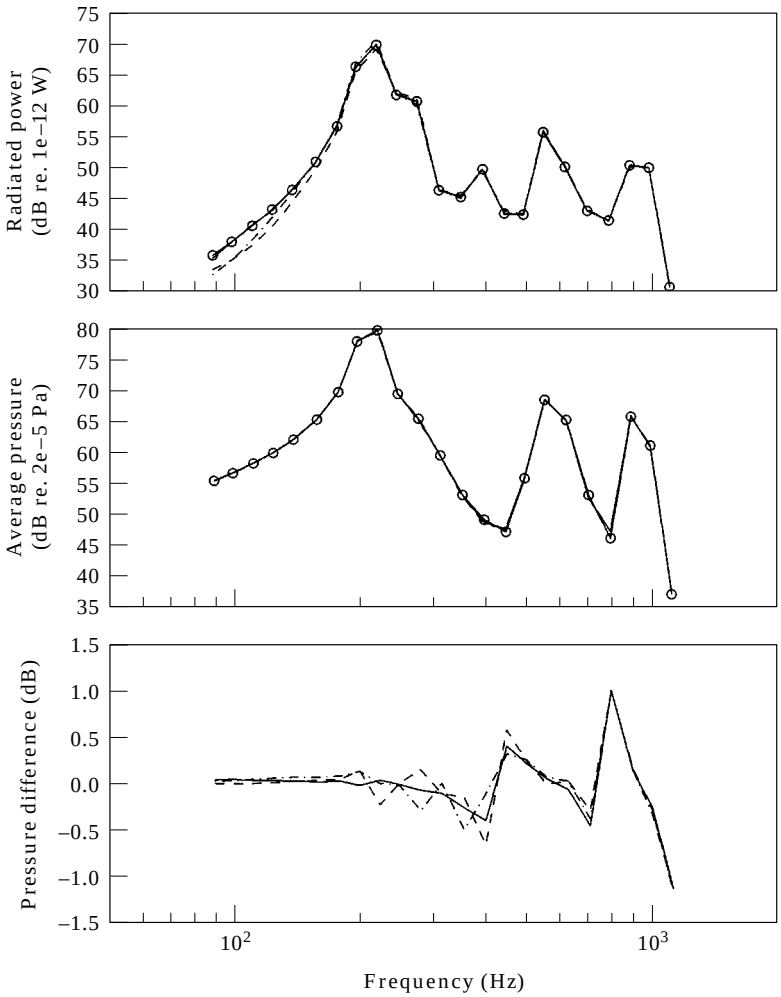

Figure 7. As Figure 6 but for $m = 1$.

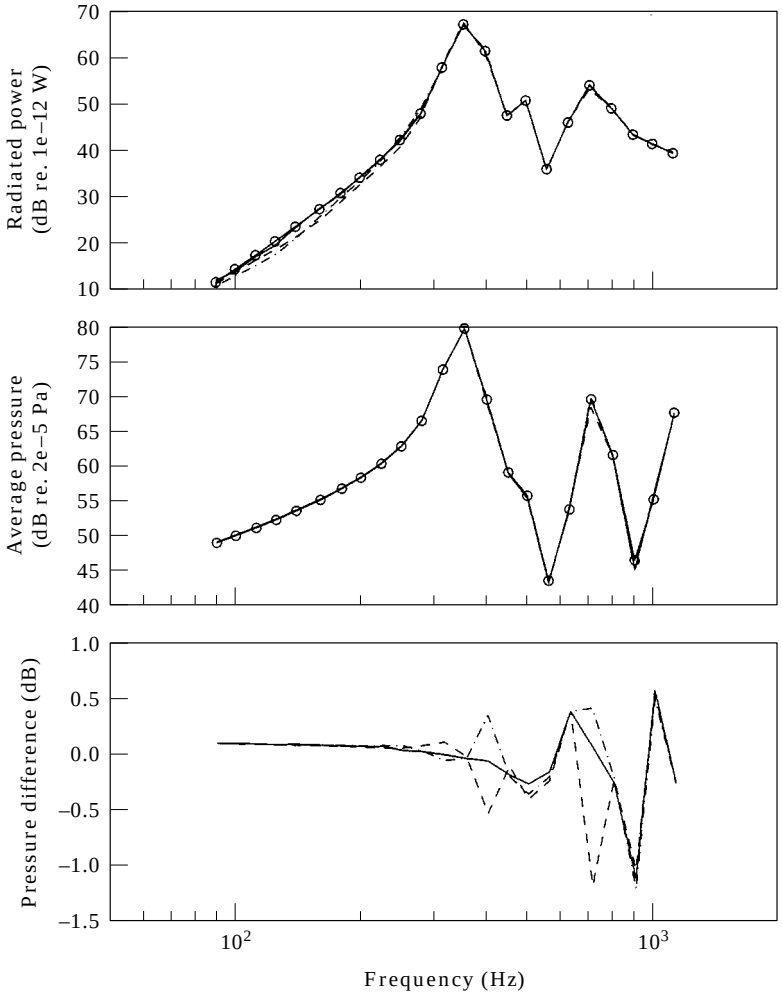

Figure 8. As Figure 6 but for $m = 2$.

Fourier–Bessel series. This is due to the fact that radiated power is associated with cut-on (i.e., propagating) modes of the acoustic field. A mode is cut-on (i.e., can propagate) if the excitation frequency is above the mode's cut-on frequency $f^c_{m\mu} \equiv j'_{m\mu}c/(2\pi a)$. If all cut-on modes are taken into account, the approximation of the radiated power will be good. In these simulations, the maximum Helmholtz number was $ka = 10$, which means that at most three cut-on modes (per Fourier

TABLE 1

Cut-on frequencies $f^c_{m\mu}$ in Hz *for acoustic duct modes*

	$\mu = 1$	$\mu = 2$	$\mu = 3$	$\mu = 4$
$m = 0$	0	418	766	1111
$m = 1$	201	582	932	
$m = 2$	333	732	1088	

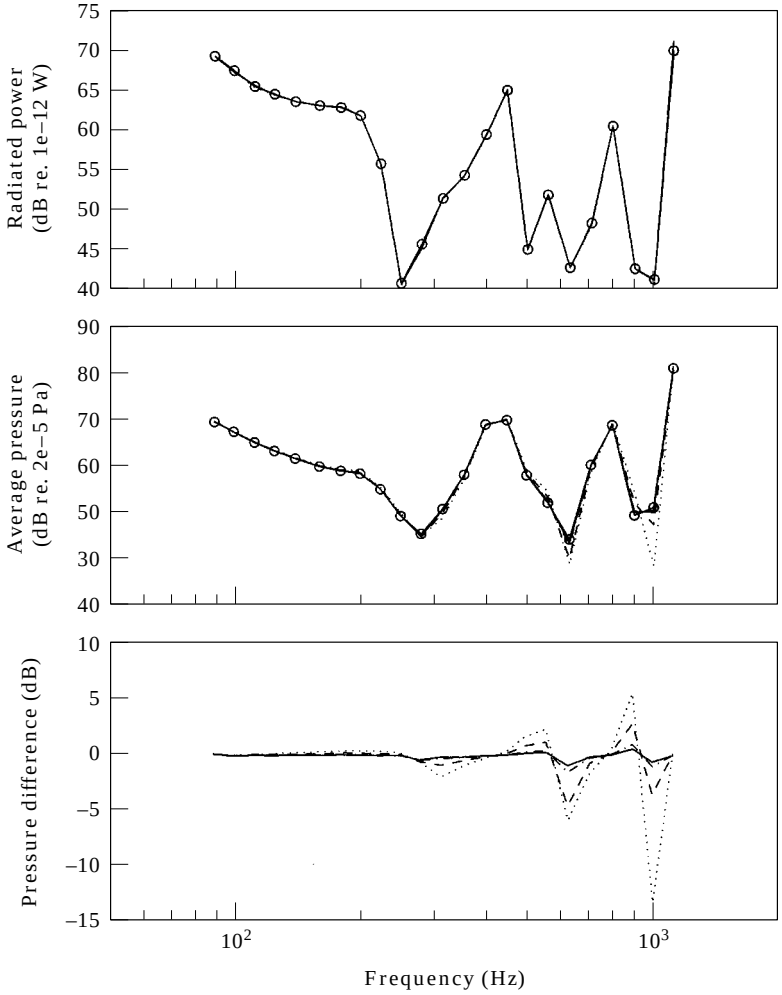

Figure 9. Acoustic responses for circumferential harmonic O for different N. Half-sine excitation. N values: · · · ·, 5; – – –, 10; · – · – · , 30; ——, 50; ○——○, FBEM.

harmonic m) were present in the acoustic field (see Table 1). This means that the computed values for the radiated power are accurate.

The results for the average pressure amplitude at the duct wall are approximated good at high pressure values, compared with the FBEM results. However, the differences at low pressure values are considerable, especially when only a few Fourier–Bessel modes are taken into account. For this model, this indicates that high pressure amplitude and radiated power values are associated with wall vibration energy being transferred to cut-on duct modes, whereas low pressure amplitude and power values are associated with vibration energy being transferred to cut-off duct modes. It is anticipated that the differences can be further minimized when the number of modes is further increased. Unfortunately, the number of modes cannot be increased infinitely because of numerical overflow and underflow errors that occur in vectors $\mathbf{h}^1$ and $\mathbf{h}^2$ for large N and consequently large values of the product $k_{m\mu}z$.

5. DISCUSSION

5.1. PHYSICAL INTERPRETATION

So-called cut-on effects dominate the acoustics of baffled finite ducts. The distinct peaks in the power and pressure spectra, located just above the cut-on frequencies of the duct are a consequence of these effects (see Figures 6–11). The cut-on peaks are caused by the large value of the "self" reflection coefficient $R_{m\mu\mu}$ of a certain duct mode (m, μ) just above its cut-on frequency. A propagating duct mode that is incident on the duct exit will almost completely be reflected because its reflection coefficient is near one. Therefore, acoustic energy that is radiated by the duct wall will build up inside the duct, much as in a closed system at resonance. This will increase the pressure at the duct wall and the net effect of that is an increase of the radiated acoustic power. This is the cause for high values for both power and average wall pressure amplitude near the cut-on frequencies of the duct. This insight can be directly attributed to the mathematics of the presented model; it would have been impossible to obtain it from just the FBEM model.

5.2. NUMERICAL EFFICIENCY

A pleasant additional property of the presented model is its numerical efficiency compared with Fourier BEM models. The computation times for both methods are dominated by the matrix assembly process. This means that if n is the number of degrees of freedom for the model, the total computational cost is of order $o(n^2)$. For the Fourier BEM model, n is the number of nodes, and for the baffled duct number n is the number of terms in the Fourier–Bessel series (N). Thus when N was increased, the computation time increased quadratically. When with constant N the Fourier harmonic number m was increased, the computation time remained almost constant. For the baffled duct model this means that the computational effort per matrix *element* is (for both methods) rather insensible on the Fourier harmonic number m or the total number of Bessel modes N.

In general, the number of degrees of freedom for a Fourier BEM model (i.e., the number of nodes) increases faster than the number of degrees of freedom for the baffled duct model (i.e., the number of terms in the Fourier–Bessel series N). When the frequency range of interest is doubled, the number of nodes for the FBEM model also needs to be doubled to obtain the same accuracy of the results. For the baffled duct model one needs only to incorporate a few more terms in the series; an additional term for every mode that was cut-off in the old frequency range and is now cut-on. This means that the computational cost will increase faster for the Fourier BEM models.

For the power radiation, an accurate approximation can be obtained with only five terms in the Fourier–Bessel series, for the baffled duct model. The approximation with five terms is almost indifferentiable from the power approximations with more terms (top graphs of Figures 9–11). For the near field pressure in the duct, the peak pressures are also approximated well with only five terms in the series. Considerable differences between the pressure results of the BD and FBEM model are only present for absolute pressure values which are at least

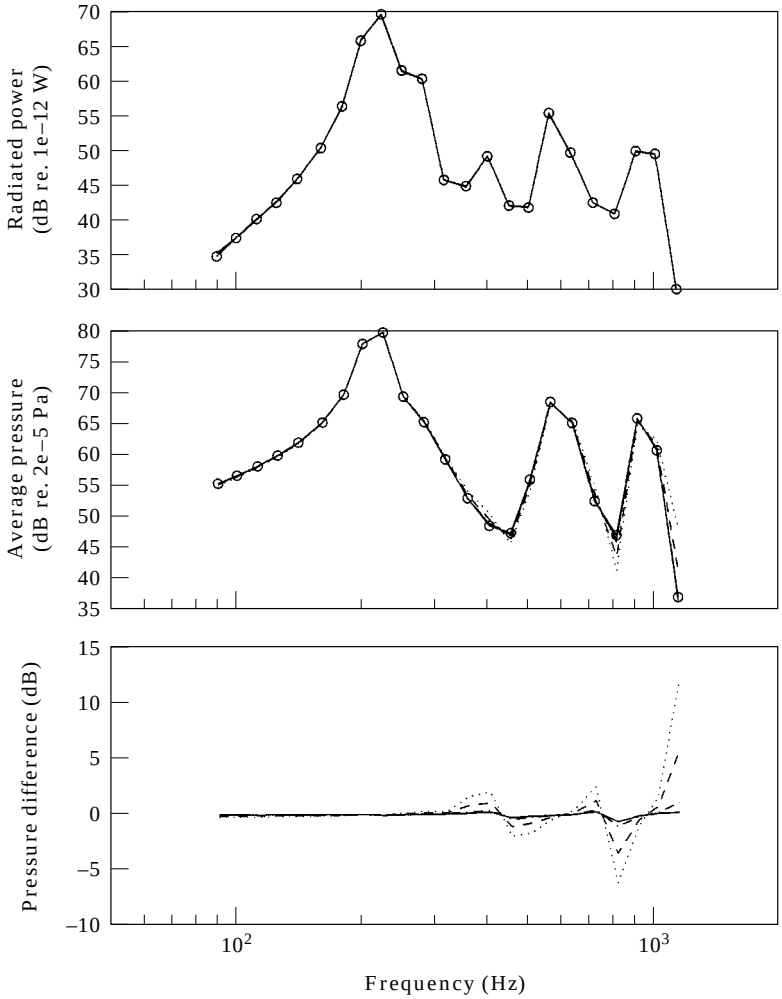

Figure 10. As Figure 9 but for $m = 1$.

25 dB below the peak pressure value, which are of lesser importance for the MRI-scanner design. This means that five terms suffice in the series of the baffled duct model when it is used for the design of the MRI scanner. Compared with the Fourier BEM model with $A = 1$ m, the five-term baffled duct model is about 15 times faster (average cpu-time per frequency, BD: 1·5 s, FBEM: 23·0 s).

6. CONCLUSIONS

A semi-analytic model for the radiation of baffled finite ducts with vibrating walls has been presented. This model can be used for the simulation of the acoustic response of MRI scanners. The acoustic response of the baffled duct models for the MRI scanner was found to be in good agreement with the response of the Fourier BEM MRI scanner models.

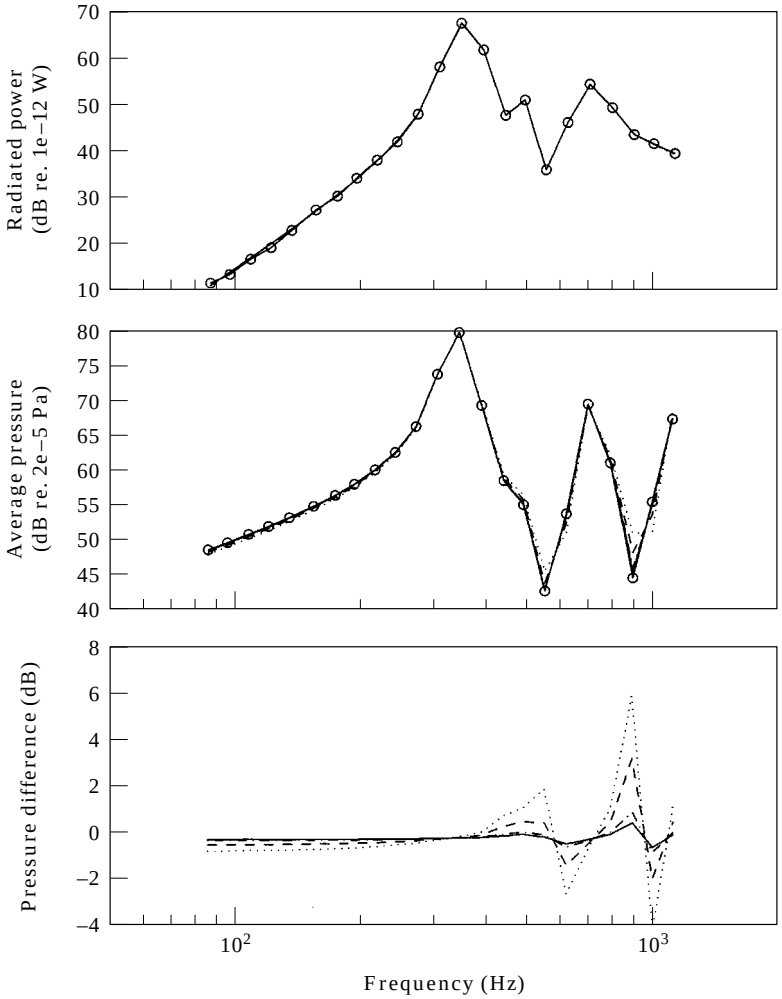

Figure 11. As Figure 9 but for $m = 2$.

The baffled duct models have two important advantages over Fourier BEM models for the design modelling of MRI scanners. First, they offer directly the relationship between important design parameters of the scanner and its acoustic response. Second, computations with the baffled duct model are about 15 times faster than computations with the Fourier BEM model, which in turn are approximately 40–500 times faster than models with commercially available three-dimensional BEM codes [e.g., reference 24].

REFERENCES

1. M. T. Vlaardingerbroek and J. Den Boer 1996 *Magnetic Resonance Imaging*. Berlin: Springer.
2. X. J. Ling, A. Amor and G. DeMeester 1995 15*th Biennial Conference on Mechanical Vibrations and Noise*, volume 84 of *Design Engineering Technical Conferences*, 311–317. Boston, MA: ASME. Numerical and experimental studies of the vibration and acoustic behaviors of MRI gradient tube.

3. B. SOENARKO 1993 *Journal of the Acoustical Society of America* **93**, 631–639. A boundary element formulation for radiation of acoustic waves from axisymmetric bodies with arbitrary boundary conditions.
4. W. WANG, N. ATALLA and J. NICOLAS 1997 *Journal of the Acoustical Society of America* **101**, 1468–1478. A boundary integral approach for acoustic radiation of axisymmetric bodies with arbitrary boundary conditions valid for all wave numbers.
5. A. H. W. M. KUIJPERS, G. VERBEEK and J. W. VERHEIJ 1997 *Journal of the Acoustical Society of America* **102**, 1394–1401. An improved acoustic Fourier boundary element method formulation using fast Fourier transform integration.
6. P. M. MORSE and K. U. INGARD 1968 *Theoretical Acoustics*. New York: McGraw-Hill.
7. E. SKUDRZYK 1971 *The Foundations of Acoustics*. Vienna: Springer-Verlag.
8. A. D. PIERCE 1981 *Acoustics*: *An Introduction to its Principles and Applications*. New York: McGraw-Hill.
9. L. E. KINSLER, A. R. FREY, A. B. COPPENS and J. V. SANDERS 1982 *Fundamentals of Acoustics*. New York: John Wiley & Sons; third edition.
10. C. L. MORFEY 1969 *Journal of Sound and Vibration* **9**, 367–372. A note on the radiation efficiency of acoustic duct modes.
11. P. E. DOAK 1973 *Journal of Sound and Vibration* **31**, 137–174. Excitation, transmission and radiation of sound from a source in a hard-walled duct of finite length, II: the effects of duct length.
12. W. E. ZORUMSKI 1973 *Journal of the Acoustical Society of America* **54**, 1667–1673. Generalized radiation impedances and reflection coefficients of circular and annular ducts.
13. K. S. WANG and T. C. TSZENG 1984 *Journal of Sound and Vibration* **93**, 57–79. Propagation and radiation of sound in a finite length duct.
14. D. A. K. HEWLETT, P. A. NELSON and C. L. MORFEY 1995 *Inter·noise* 95, 1333–1336. An exact solution for the acoustic radiation from a finite length circular duct.
15. B. E. SANDMAN 1976 *Journal of the Acoustical Society of America* **60**, 1256–1264. Fluid loading influence coefficients for a finite cylindrical shell.
16. A. HARARI and B. E. SANDMAN 1976 *Journal of the Acoustical Society of America* **60**, 117–128. Vibratory response of laminated cylindrical shells embedded in an acoustic fluid.
17. P. J. T. FILIPPI and D. HABAULT 1989 *Journal of Sound and Vibration* **131**, 13–23. Sound radiation by a baffled cylindrical shell: a numerical technique based on boundary integral equations. Part 1.
18. D. HABAULT and P. J. T. FILIPPI 1989 *Journal of Sound and Vibration* **131**, 25–36. Sound radiation by a baffled cylindrical shell: a numerical technique based on boundary integral equations. Part 2.
19. K. GROSH, P. M. PINSKY, M. MALHOTRA and V. S. RAO 1994 *International Journal for Numerical Methods in Engineering* **37**, 2971–2985. Finite element formulation for a baffled, fluid-loaded finite cylindrical shell.
20. S. H. CHOI, T. IGUSA and J. D. ACHENBACH 1996 *Journal of Sound and Vibration* **197**, 329–350. Acoustic radiation from a finite-length shell with non-axisymmetric substructures using a surface variational principle.
21. G. N. WATSON 1966 *A Treatise on the Theory of Bessel functions*. Cambridge: Cambridge University Press; second edition.
22. E. KREYSZIG 1993 *Advanced Engineering Mathematics*. New York: John Wiley & Sons; seventh edition.
23. A. H. W. M. KUIJPERS 1997 *bARD v2.8 manual*. Computational and experimental mechanics. Eindhoven, The Netherlands: Eindhoven University of Technology.
24. LMS NUMERICAL TECHNOLOGIES 1996 *SYSNOISE R5.3 On-Line Documentation*. Leuven, Belgium.

APPENDIX A: GENERALIZED RADIATION IMPEDANCES

The pressure and velocity at the exit of a finite duct that terminates in an infinite flange can be written as (see section 2.5.1)

$$p(r_e, \theta_e, z_e) = \sum_{m=-\infty}^{\infty} \mathrm{e}^{-\mathrm{i}m\theta_e} \sum_{\mu=1}^{\infty} P_{m\mu} \mathrm{J}_m(\alpha_{m\mu} r_e), \tag{A1}$$

$$u_z(r_e, \theta_e, z_e) = \frac{1}{\rho_0 c_0} \sum_{m=-\infty}^{\infty} \mathrm{e}^{-\mathrm{i}m\theta_e} \sum_{\mu=1}^{\infty} V_{m\mu} \mathrm{J}_m(\alpha_{m\mu} r_e), \tag{A2}$$

with co-ordinates $\mathbf{x}_e = (r_e, \theta_e, z_e)$ for a point a the duct's exit. The pressure at a point $\mathbf{x} = (r, \theta, z)$ outside the duct ($z \leqslant -L$ or $z \geqslant L$) is given by the Rayleigh integral which depends on the (axial) velocity at the duct exit,

$$p(\mathbf{x}) = \frac{\mathrm{i}\rho_0 \omega}{2\pi} \int_{S_e} u_z(\mathbf{x}_e) \frac{\mathrm{e}^{-\mathrm{i}kR(\mathbf{x}, \mathbf{x}_e)}}{R(\mathbf{x}, \mathbf{x}_e)} \, \mathrm{d}S, \tag{A3}$$

where

$$R(\mathbf{x}, \mathbf{x}_e) = \|\mathbf{x} - \mathbf{x}_e\| = [r^2 + r_e^2 - 2rr_e \cos(\theta - \theta_e) + (z - z_e)^2]^{\frac{1}{2}} \tag{A4}$$

is the distance between the point outside the duct and a point in the duct's exit, and S_e is the cross-section of the duct's exit. The expression for $u_z(\mathbf{x}_e)$ from equation (A2) can be substituted into the Rayleigh integral to obtain

$$p(r, \theta, z) = \frac{\mathrm{i}k}{2\pi} \int_0^{2\pi} \int_0^a \sum_{m=-\infty}^{\infty} \mathrm{e}^{-\mathrm{i}m\theta_e} \sum_{\mu=1}^{\infty} V_{m\mu} \mathrm{J}_m(\alpha_{m\mu} r_e) \frac{\mathrm{e}^{-\mathrm{i}kR}}{R} r_e \, \mathrm{d}r_e \, \mathrm{d}\theta_e. \tag{A5}$$

For further manipulation it is convenient to eliminate the function of R in equation (A5). Sonine's infinite integral [21, p. 416, equation (4), with Im $(\sqrt{1-\tau^2}) \leqslant 0$ and the complex integration contour passes above the real axis], is introduced:

$$\frac{\mathrm{e}^{-\mathrm{i}kR}}{-\mathrm{i}kR} = \int_0^{\infty} \frac{\tau}{\sqrt{1-\tau^2}} \mathrm{J}_0(\tau kR) \, \mathrm{d}\tau. \tag{A6}$$

The Bessel function in equation (A6) may be replaced, at the duct's exit ($z = z_e$ and thus $R = R(r, \theta, r_e, \theta_e)$), by use of Neumann's addition theorem [21, p. 358, equation (1)]:

$$\mathrm{J}_0(\tau kR) = \sum_{m=-\infty}^{\infty} \mathrm{J}_m(\tau kr) \mathrm{J}_m(\tau kr_e) \, \mathrm{e}^{-\mathrm{i}m(\theta - \theta_e)}. \tag{A7}$$

Substituting equation (A7) in equation (A6) results in

$$\frac{\mathrm{e}^{-\mathrm{i}kR}}{R} = -\mathrm{i}k \sum_{m=-\infty}^{\infty} \mathrm{e}^{-\mathrm{i}m(\theta - \theta_e)} \int_0^{\infty} \frac{\tau}{\sqrt{1-\tau^2}} \mathrm{J}_m(\tau kr) \mathrm{J}_m(\tau kr_e) \, \mathrm{d}\tau. \tag{A8}$$

With this result, equation (A5) (at $z = z_e$) can now be expressed as

$$p(r, \theta, z_e) = k \sum_{m=-\infty}^{\infty} \mathrm{e}^{-\mathrm{i}m\theta} \sum_{\mu=1}^{\infty} V_{m\mu} \int_0^{\infty} \frac{\tau}{\sqrt{1-\tau^2}} \mathrm{J}_m(\tau k r) D_{m\mu}(\tau)\, \mathrm{d}\tau, \tag{A9}$$

where the integration over angle θ_e has been performed and function $D_{m\mu}(\tau)$ is given by

$$D_{m\mu}(\tau) = k \int_0^a \mathrm{J}_m(\tau k r) \mathrm{J}_m(\alpha_{m\mu} r) r\, \mathrm{d}r. \tag{A10}$$

The integral $D_{m\mu}(\tau)$ may be evaluated directly [21, p. 134, equation (8)]:

$$D_{m\mu}(\tau) = \frac{\tau k^2 a}{\tau^2 k^2 - \alpha_{m\mu}^2} \mathrm{J}'_m(\tau k a) \mathrm{J}_m(\alpha_{m\mu} a). \tag{A11}$$

Equation (A1) can now be equated to equation (A9) to obtain

$$\sum_{m=-\infty}^{\infty} \mathrm{e}^{-\mathrm{i}m\theta} \sum_{\mu=1}^{\infty} P_{m\mu} \mathrm{J}_m(\alpha_{m\mu} r) = k \sum_{n=-\infty}^{\infty} \mathrm{e}^{-\mathrm{i}n\theta} \sum_{\nu=1}^{\infty} V_{n\nu} \int_0^{\infty} \frac{\tau}{\sqrt{1-\tau^2}} \mathrm{J}_n(\tau k r) D_{n\nu}(\tau)\, \mathrm{d}\tau. \tag{A12}$$

Multiplying both sides of this equation by $\mathrm{e}^{\mathrm{i}p\theta} \mathrm{J}_p(\alpha_{p\xi} r)$ and integrating over the duct cross-section while exchanging the summation and integration operators gives

$$\sum_{m=-\infty}^{\infty} \sum_{\mu=1}^{\infty} P_{m\mu} \int_0^{2\pi} \int_0^a \mathrm{J}_m(\alpha_{m\mu} r)\, \mathrm{e}^{-\mathrm{i}m\theta} \mathrm{J}_p(\alpha_{p\xi} r)\, \mathrm{e}^{\mathrm{i}p\theta} r\, \mathrm{d}r\, \mathrm{d}\theta$$

$$= k \sum_{n=-\infty}^{\infty} \sum_{\nu=1}^{\infty} V_{n\nu} \int_0^{\infty} \frac{\tau}{\sqrt{1-\tau^2}} \int_0^{2\pi} \int_0^a \mathrm{J}_n(\tau k r)\, \mathrm{e}^{-\mathrm{i}n\theta} \mathrm{J}_p(\alpha_{p\xi} r)\, \mathrm{e}^{\mathrm{i}p\theta} r\, \mathrm{d}r\, \mathrm{d}\theta\, D_{n\nu}(\tau)\, \mathrm{d}\tau. \tag{A13}$$

The orthogonality property for the modes in radial and circumferential direction gives for the left side of equation (A13) (where $\alpha_{m\mu}$ and $\alpha_{p\xi}$ are zeros of $J'_m(\alpha a)$, $J'_p(\alpha a)$, respectively:

$$\int_0^{2\pi} \int_0^a \mathrm{J}_m(\alpha_{m\mu} r)\, \mathrm{e}^{-\mathrm{i}m\theta} \mathrm{J}_p(\alpha_{p\xi} r)\, \mathrm{e}^{\mathrm{i}p\theta} r\, \mathrm{d}r\, \mathrm{d}\theta$$

$$= \delta_{mp} \delta_{\mu\xi} \pi (a^2 - m^2/\alpha_{m\mu}^2) \mathrm{J}_m(\alpha_{m\mu} a)^2$$

$$= \delta_{mp} \delta_{\mu\xi} 2\pi N_{m\mu}^2 \quad \text{for } m = 0, \pm 1, \pm 2, \ldots, \quad \text{and for } \mu = 1, 2, \ldots. \tag{A14}$$

The amplitudes of each pressure mode at the duct's exit are then given by

$$P_{m\mu} = \frac{k}{N_{m\mu}^2} \sum_{v=1}^{\infty} V_{mv} \int_0^{\infty} \frac{\tau}{\sqrt{1-\tau^2}} \int_0^a \mathrm{J}_m(\tau kr)\mathrm{J}_m(\alpha_{m\mu} r) r \, \mathrm{d}r \, D_{mv}(\tau) \, \mathrm{d}\tau,$$

which can be further simplified by using the definition for $D_{m\mu}(\tau)$ to obtain

$$P_{m\mu} = \sum_{v=1}^{\infty} \frac{V_{mv}}{N_{m\mu}^2} \int_0^{\infty} \frac{\tau}{\sqrt{1-\tau^2}} D_{m\mu}(\tau) D_{mv}(\tau) \, \mathrm{d}\tau. \tag{A15}$$

Equation (A15) may be used to express the modal impedance given by

$$P_{m\mu} = \sum_{v=1}^{\infty} Z_{m\mu v} V_{mv}, \quad \text{for } m = 0, \pm 1, \pm 2, \ldots, \quad \text{and for } \mu = 1, 2, \ldots, \tag{A16}$$

where

$$Z_{m\mu v} = \frac{1}{N_{m\mu}^2} \int_0^{\infty} \frac{\tau}{\sqrt{1-\tau^2}} D_{m\mu}(\tau) D_{mv}(\tau) \, \mathrm{d}\tau, \tag{A17}$$

and the boundary conditions are satisfied such that $\mathrm{J}'(\alpha_{m\mu} a) = 0$.

APPENDIX B: COMPUTATION OF GENERALIZED RADIATION IMPEDANCES

To compute the integral in equation (A17), Zorumski [12] suggested splitting up the integration range in a part $\tau \in [0, 1]$ and $\tau \in [1, \infty]$. By using change of variables $\tau = \sin \phi$ for the first range and $\tau = \cosh \psi$ for the second, the expression for the generalized modal impedance becomes

$$Z_{m\mu v} = \frac{1}{N_{m\mu}^2} \int_0^{\frac{1}{2}\pi} \sin \phi D_{m\mu}(\sin \phi) D_{mv}(\sin \phi) \, \mathrm{d}\phi$$

$$+ \frac{\mathrm{i}}{N_{m\mu}^2} \int_0^{\infty} \cosh \psi D_{m\mu}(\cosh \psi) D_{mv}(\cosh \psi) \, \mathrm{d}\psi. \tag{B1}$$

At first sight this seems to be an elegant solution since the integral is split up in a real and imaginary part, and the singularity for $\tau = 1$ has been removed by the transformation. However, because of the oscillatory nature of the function $D_{m\mu}(\tau)$, numerical evaluation of the integral is very expensive. To make things worse, the oscillatory behavior of the integrand is blown up by the cosh (ψ) argument of the function $D_{m\mu}(\tau)$. In brief, the transformations suggested by Zorumski [12] do not offer a numerically workable expression for the generalized radiation impedances

and therefore an alternative, numerically more attractive expression will be derived here.

For further manipulation it is convenient to write out $Z_{m\mu\nu}$ as

$$Z_{m\mu\nu} = \frac{2\alpha_{m\mu}^2 a^2 \mathrm{J}_m(\alpha_{m\nu}a)}{(\alpha_{m\mu}^2 a^2 - m^2)\mathrm{J}_m(\alpha_{m\mu}a)} \int_0^\infty \frac{\tau^3 \mathrm{J}'_m(\tau ka)^2}{\sqrt{1-\tau^2}\left(\tau^2 - \frac{\alpha_{m\mu}^2}{k^2}\right)\left(\tau^2 - \frac{\alpha_{m\nu}^2}{k^2}\right)} \mathrm{d}\tau. \tag{B2}$$

Note that $\mathrm{J}'_m(\tau ka)/(\tau^2 - \alpha_{m\mu}^2/k^2)$ is analytic (even at $\tau = \alpha_{m\mu}/k$). Equation (B2) can be rewritten to

$$Z_{m\mu\nu} = E_{m\mu\nu} \int_0^\infty F_{m\mu\nu}(\tau)[\mathrm{H}_m^{(1)'}(\tau ka) + \mathrm{H}_m^{(2)'}(\tau ka)]\, \mathrm{d}\tau, \tag{B3}$$

with Hankel functions

$$\mathrm{H}_m^{(1)}(x) = \mathrm{J}_m(x) + \mathrm{i}\mathrm{Y}_m(x), \qquad \mathrm{H}_m^{(2)}(x) = \mathrm{J}_m(x) - \mathrm{i}\mathrm{Y}_m(x), \tag{B4, B5}$$

$$E_{m\mu\nu} = 2\alpha_{m\mu}^2 a^2 \mathrm{J}_m(\alpha_{m\nu}a)/(\alpha_{m\mu}^2 a^2 - m^2)\mathrm{J}_m(\alpha_{m\mu}a), \tag{B6}$$

and

$$F_{m\mu\nu}(\tau) = \frac{1}{2}\frac{\tau^3}{\sqrt{1-\tau^2}} \frac{1}{(\tau + \alpha_{m\mu}/k)(\tau + \alpha_{m\nu}/k)} \frac{\mathrm{J}'_m(\tau ka)}{(\tau - \alpha_{m\mu}/k)(\tau - \alpha_{m\nu}/k)}. \tag{B7}$$

The function $F_{m\mu\nu}(\tau)$ is analytic, except for the case $\mu = \nu$ when the poles coincide. Rewriting equation (B3) yields

$$Z_{m\mu\nu} = E_{m\mu\nu}\left[\fint_0^\infty F_{m\mu\nu}(\tau)\mathrm{H}_m^{(1)'}(\tau ka)\, \mathrm{d}\tau + \fint_0^\infty F_{m\mu\nu}(\tau)\mathrm{H}_m^{(2)'}(\tau ka)\, \mathrm{d}\tau \right] \tag{B8}$$

$$= E_{m\mu\nu}[Z_{m\mu\nu}^{(1)} + Z_{m\mu\nu}^{(2)}], \tag{B9}$$

where $\fint$ denotes that the integration path is deformed and passes above the pole $\tau = \alpha_{m\mu}/k$ for $\mu = \nu$. These integrals can be computed by using contour deformation in the complex plane. With the help of the equations

$$\mathrm{H}_m^{(1)'}(\mathrm{i}x) = \frac{2}{\pi}(-\mathrm{i})^{m+2}\mathrm{K}'_m(x), \qquad \arg(x) \in (-\pi, \tfrac{1}{2}\pi], \tag{B10}$$

$$\mathrm{H}_m^{(2)'}(-\mathrm{i}x) = \frac{2}{\pi}(\mathrm{i})^{m+2}\mathrm{K}'_m(x), \qquad \arg(x) \in (-\tfrac{1}{2}\pi, \pi], \tag{B11}$$

with the modified Hankel function

$$K_m(x) = \begin{Bmatrix} \frac{1}{2}\pi i^{m+1} H_m^{(1)}(ix), & \arg(x) \in (-\pi, \frac{1}{2}\pi] \\ \frac{1}{2}\pi i^{m+1} H_m^{(1)}(ix) - 2\pi i(-1)^m I_m(x), & \arg(x) \in (\frac{1}{2}\pi, \pi] \end{Bmatrix} \tag{B12}$$

$$= \begin{Bmatrix} \frac{1}{2}\pi(-i)^{m+1} H_m^{(2)}(-ix), & \arg(x) \in (-\frac{1}{2}\pi, \pi] \\ \frac{1}{2}\pi(-i)^{m+1} H_m^{(2)}(-ix) + 2\pi i(-1)^m I_m(x), & \arg(x) \in (-\pi, -\frac{1}{2}\pi] \end{Bmatrix}, \tag{B13}$$

and with the modified Bessel function of the first kind

$$I_m(x) = i^{-m} J_m(ix), \tag{B14}$$

the components of equation (B9) can be written as

$$Z_{m\mu\nu}^{(1)} = \int_0^\infty F_{m\mu\nu}(i\tau) \frac{2}{\pi} (-i)^{m+1} K_m'(\tau ka)\, d\tau, \tag{B15}$$

$$Z_{m\mu\nu}^{(2)} = 2 \int_0^1 F_{m\mu\nu}(\tau) H_m^{(2)'}(\tau ka)\, d\tau + \int_0^\infty F_{m\mu\nu}(-i\tau) \frac{2}{\pi} i^{m+1} K_m'(\tau ka)\, d\tau$$

$$+ \delta_{\mu\nu} 2\pi i \operatorname*{Res}_{t = \alpha_{m\mu}/k} F_{m\mu\mu}(\tau) H_m^{(2)'}(\tau ka). \tag{B16}$$

Combining these terms yields

$$Z_{m\mu\nu} = 2E_{m\mu\nu} \left[\int_0^1 F_{m\mu\nu}(\tau) H_m^{(2)'}(\tau ka)\, d\tau + \frac{i}{\pi} \int_0^\infty \frac{\tau^3 I_m'(\tau ka) K_m'(\tau ka)}{\sqrt{1+\tau^2}\left(\tau^2 + \frac{\alpha_{m\mu}^2}{k^2}\right)\left(\tau^2 + \frac{\alpha_{m\nu}^2}{k^2}\right)} d\tau \right.$$

$$\left. + \delta_{\mu\nu} \pi i \operatorname*{Res}_{\tau = \alpha_{m\mu}/k} F_{m\mu\mu}(\tau) H_m^{(2)'}(\tau ka) \right]. \tag{B17}$$

The singularity in $F_{m\mu\nu}(\tau)$ for $\tau = 1$ in equation (B17) can be removed by substituting $\tau = \sin(\theta)$:

$$\int_0^1 \frac{\tau^3}{2\sqrt{1-\tau^2}} \frac{J_m'(\tau ka) H_m^{(2)'}(\tau ka)}{(\tau^2 - \alpha_{m\mu}^2/k^2)(\tau^2 - \alpha_{m\nu}^2/k^2)} d\tau$$

$$= \int_0^{\frac{1}{2}\pi} \frac{\sin^3(\theta) J_m'(\sin(\theta) ka) H_m^{(2)'}(\sin(\theta) ka)}{2(\sin^2(\theta) - \alpha_{m\mu}^2/k^2)(\sin^2(\theta) - \alpha_{m\nu}^2/k^2)} d\theta. \tag{B18}$$

The infinite integral in equation (B17) can be transformed to two finite integrals by splitting the integration interval $[0, \infty]$ into $[0, 1]$ and $[1, \infty]$ and using the substitution $t = 1/\tau$ for the second interval:

$$\int_0^\infty \frac{\tau^3 \mathrm{I}'_m(\tau ka)\mathrm{K}'_m(\tau ka)}{\sqrt{1+\tau^2}\left(\tau^2 + \frac{\alpha_{m\mu}^2}{k^2}\right)\left(\tau^2 + \frac{\alpha_{mv}^2}{k^2}\right)} \mathrm{d}\tau = \int_0^1 \frac{\tau^3 \mathrm{I}'_m(\tau ka)\mathrm{K}'_m(\tau ka)}{\sqrt{1+\tau^2}\left(\tau^2 + \frac{\alpha_{m\mu}^2}{k^2}\right)\left(\tau^2 + \frac{\alpha_{mv}^2}{k^2}\right)} \mathrm{d}\tau$$

$$+ \int_0^1 \frac{\mathrm{I}'_m(ka/t)\mathrm{K}'_m(ka/t)}{\sqrt{t^2+1}\left(1 + \frac{\alpha_{m\mu}^2 t^2}{k^2}\right)\left(1 + \frac{\alpha_{mv}^2 t^2}{k^2}\right)} \mathrm{d}t. \tag{B19}$$

With limits

$$\lim_{x\to 0} x^2 \mathrm{I}'_m(x)\mathrm{K}'_m(x) = \begin{cases} -\frac{1}{2}x^2 & \text{for } m = 0 \\ -\frac{1}{2}n & \text{for } m \geqslant 1 \end{cases}, \qquad \lim_{x\to\infty} \mathrm{I}'_m(x)\mathrm{K}'_m(x) = 0, \tag{B20, B21}$$

it can be shown that the first integrand approaches zero for $\tau \to 0$, and that the second integrand also approaches zero for $t \to 0$.

When $\mu = v$ the residue at pole $\tau = \alpha_{m\mu} = \alpha_{mv}$ has to be taken into account. Four cases can be distinguished: (1) the pole is not on the branch of $1/\sqrt{1-\tau^2}$; (2) the pole lies on the branch of $1/\sqrt{1-\tau^2}$, but not in 0 or 1; (3) the pole lies at $\tau = 0$; (4) the pole lies at $\tau = 1$.

In case (1) $\tau > 1$ or $\alpha_{m\mu}/k = \alpha_{mv}/k > 1$. This means that the free field wavenumber k is smaller than radial wavenumber $\alpha_{m\mu}$, in other words, the mode is cut-off (evanescent). The residue at this pole is

$$\operatorname*{Res}_{\tau = \alpha_{m\mu}/k} E_{m\mu\mu} F_{m\mu\mu}(\tau)\mathrm{H}_m^{(2)'}(\tau ka) = \frac{E_{m\mu\mu}(\alpha_{m\mu}^2 a^2 - m^2)}{4\pi\alpha_{m\mu}^2 a^2 \sqrt{(\alpha_{m\mu}/k)^2 - 1}}. \tag{B22}$$

In case (2) $0 < \tau < 1$ or $0 < \alpha_{m\mu}/k < 1$ the pole lies on the branch of $1/\sqrt{1-\tau^2}$. This means that the free field wavenumber k is larger than radial wavenumber $\alpha_{m\mu}$, in other words, the mode is cut-on (propagating). The pole is not inside the integration contour, and it can be shown that it has no contribution to the modal impedance. However, the finite integral in equation (B17) must then be interpreted as a Cauchy Principal Value integral:

$$Z_{m\mu\mu} = 2E_{m\mu\mu}\left[\mathrm{CPV}\int_0^1 F_{m\mu\mu}(\tau)\mathrm{H}_m^{(2)'}(\tau ka)\,\mathrm{d}\tau + \frac{\mathrm{i}}{\pi}\int_0^\infty \frac{\tau^3 \mathrm{I}'_m(\tau ka)\mathrm{K}'_m(\tau ka)}{\sqrt{1+\tau^2}\left(\tau^2 + \frac{\alpha_{m\mu}^2}{k^2}\right)^2}\,\mathrm{d}\tau\right]. \tag{B23}$$

In case (3) the pole lies on $\tau = \alpha_{m\mu}/k = 0$. This can happen only for the plane wave mode ($m = 0$, $\mu = \nu = 1$ and $\alpha_{01} = 0$). The modal impedance is then defined as

$$Z_{011} = 2E_{011} \int_0^\infty \frac{J_1^2(\tau ka)}{2\tau\sqrt{1-\tau^2}}\,d\tau. \tag{B24}$$

The identity $J_1(x) = \frac{1}{2}[H_1^{(1)}(x) + H_1^{(2)}(x)]$ is used to transform the integral in equation (B24) into

$$Z_{011} = E_{011} \lim_{\epsilon\to 0}\left[\int_\epsilon^\infty \frac{J_1(\tau ka)H_1^{(1)}(\tau ka)}{2\tau\sqrt{1-\tau^2}}\,d\tau + \int_\epsilon^\infty \frac{J_1(\tau ka)H_1^{(2)}(\tau ka)}{2\tau\sqrt{1-\tau^2}}\,d\tau\right]. \tag{B25}$$

Deformation of the complex integration path similar to the derivation used for equation (B9) can be used. It can be shown that the pole at $\tau = 0$ has no contribution. The resulting expression for the modal "self" impedance of the plane wave,

$$Z_{011} = 2E_{011} \lim_{\epsilon\to 0}\left[2\int_\epsilon^1 \frac{J_1(\tau ka)H_1^{(2)}(\tau ka)}{2\tau\sqrt{1-\tau^2}}\,d\tau - \frac{i}{\pi}\int_\epsilon^\infty \frac{I_1(\tau ka)K_1(\tau ka)}{\tau\sqrt{1+\tau^2}}\,d\tau\right], \tag{B26}$$

contains two integrals whose integrands are singular for $\varepsilon\to 0$, but their contributions cancel each other. Therefore, it is convenient to combine the integrands in the region $\tau\in[0, 1]$:

$$Z_{011} = 2E_{011}\left\{\int_0^1 \left[\frac{J_1(\tau ka)H_1^{(2)}(\tau ka)}{2\tau\sqrt{1-\tau^2}} - \frac{i}{\pi}\frac{I_1(\tau ka)K_1(\tau ka)}{\tau\sqrt{1+\tau^2}}\right]d\tau\right.$$

$$\left. - \frac{i}{\pi}\int_1^\infty \frac{I_1(\tau ka)K_1(\tau ka)}{\tau\sqrt{1+\tau^2}}\,d\tau\right\}. \tag{B27}$$

The singularity in the first integrand for $\tau = 1$ can be removed by substituting $\tau = \sin(\theta)$ and the second integral can be transformed into a finite integral by substituting $\tau = 1/t$. Thus, the modal impedance is defined by

$$Z_{011} = 2E_{011}\left\{\int_0^{\frac{1}{2}\pi} \left[\frac{J_1(ka\sin\theta)H_1^{(2)}(ka\sin\theta)}{2\sin\theta} - \frac{i}{\pi}\frac{I_1(ka\sin\theta)K_1(ka\sin\theta)\cos\theta}{\sin\theta\sqrt{1+\sin^2\theta}}\right]d\theta\right.$$

$$\left. - \frac{i}{\pi}\int_0^1 \frac{I_1(ka/t)K_1(ka/t)}{\sqrt{t^2+1}}\,dt\right\}. \tag{B28}$$

In case (4) the pole lies on $\tau = \alpha_{m\mu}/k = 1$. This means that the free field wavenumber k equals the radial wavenumber $\alpha_{m\mu}$. The axial wavenumber: $k_{m\mu} = \sqrt{(k^2 - \alpha_{m\mu}^2)}$ then equals zero. Physically, this occurs at duct mode resonance frequencies which are not studied here.

APPENDIX C: RADIATED ACOUSTIC POWER

To compute the time averaged power radiated by the baffled finite duct, the time average of the acoustic normal intensity $\bar{\mathbf{I}} \cdot \mathbf{n}$ has to be integrated over a surface that surrounds the duct,

$$\bar{P} = \int_S \bar{\mathbf{I}} \cdot \mathbf{n} \, \mathrm{d}S, \tag{C1}$$

with surface S, $\mathbf{I} = p\mathbf{u}$ as the acoustic energy flux vector, and $\mathbf{n}$ as the unit normal vector. The bar notation denotes the time average.

C.1. DUCT WALL POWER RADIATION

The radiated power by the duct can be computed by integrating the time averaged product of acoustic pressure p and normal velocity u_r over the duct wall surface:

$$\bar{P} = -\tfrac{1}{2} \operatorname{Re} \int_{-L}^{L} \int_{0}^{2\pi} p(a, \theta, z) u_r^*(a, \theta, z) a \, \mathrm{d}\theta \, \mathrm{d}z, \tag{C2}$$

where * denotes the complex conjugate. By using equation (36) for pressure p and equation (20) for normal velocity u_r the following expression for the acoustic normal intensity at the duct wall can be derived:

$$\bar{\mathbf{I}} \cdot \mathbf{n} = \frac{1}{2\pi} \sum_{m=-\infty}^{\infty} \mathrm{e}^{-\mathrm{i}m\theta} \sum_{n=-\infty}^{\infty} \eta_n^*(z) \, \mathrm{e}^{\mathrm{i}n\theta} \sum_{\mu=1}^{\infty} \mathrm{J}_m(\alpha_{m\mu} a) \left[A_{m\mu}(z) \, \mathrm{e}^{-\mathrm{i}k_{m\mu} z} + B_{m\mu}(z) \, \mathrm{e}^{\mathrm{i}k_{m\mu} z} \right]. \tag{C3}$$

Integrating this expression over the duct wall surface yields

$$\bar{P} = \tfrac{1}{2} a \operatorname{Re} \sum_{m=-\infty}^{\infty} \sum_{\mu=1}^{\infty} \mathrm{J}_m(\alpha_{m\mu} a) \int_{-L}^{L} \eta_m^*(z) \left[A_{m\mu}(z) \, \mathrm{e}^{-\mathrm{i}k_{m\mu} z} + B_{m\mu}(z) \, \mathrm{e}^{\mathrm{i}k_{m\mu} z} \right] \mathrm{d}z. \tag{C4}$$

C.2. DUCT EXIT POWER RADIATION

The transmitted power in the axial (positive z) direction P_z over a duct cross-section can be computed by integrating the time averaged product of acoustic pressure p and axial velocity u_z over the duct cross-section:

$$\bar{P}_z(z_0) = \tfrac{1}{2}\,\mathrm{Re}\int_0^a\int_0^{2\pi} p(r,\theta,z_0)u_z^*(r,\theta,z_0)r\,\mathrm{d}\theta\,\mathrm{d}r. \tag{C5}$$

By using equation (36) for pressure p, and

$$u_z(r,\theta,z_0) = \sum_{m=-\infty}^{\infty}\sum_{\mu=1}^{\infty} \mathrm{J}_m(\alpha_{m\mu}r)\,\mathrm{e}^{-\mathrm{i}m\theta}\,\frac{k_{m\mu}}{\rho_0 c_0 k}\,(A_{m\mu}(z_0)\,\mathrm{e}^{-\mathrm{i}k_{m\mu}z_0} - B_{m\mu}(z_0)\,\mathrm{e}^{\mathrm{i}k_{m\mu}z_0}) \tag{C6}$$

for axial velocity u_z, the following expression for the acoustic axial intensity at the duct exit can be derived:

$$\begin{aligned}\bar{\mathbf{I}}\cdot\mathbf{e}_z = \sum_{m=-\infty}^{\infty}\sum_{n=-\infty}^{\infty}\sum_{\mu=1}^{\infty}\sum_{\nu=1}^{\infty} \mathrm{e}^{-\mathrm{i}m\theta}\,\mathrm{e}^{\mathrm{i}n\theta}\mathrm{J}_m(\alpha_{m\mu}r)\mathrm{J}_n(\alpha_{n\nu}r)\,\frac{k_{n\nu}^*}{k\rho_0 c_0}\\ \times\,[A_{m\mu}(z_0)A_{n\nu}^*(z_0)\,\mathrm{e}^{-\mathrm{i}(k_{m\mu}-k_{n\nu}^*)z_0} - A_{m\mu}(z_0)B_{n\nu}^*(z_0)\,\mathrm{e}^{-\mathrm{i}(k_{m\mu}+k_{n\nu}^*)z_0}\\ +\,B_{m\mu}(z_0)A_{n\nu}^*(z_0)\,\mathrm{e}^{\mathrm{i}(k_{m\mu}+k_{n\nu}^*)z_0} - B_{m\mu}(z_0)B_{n\nu}^*(z_0)\,\mathrm{e}^{\mathrm{i}(k_{m\mu}-k_{n\nu}^*)z_0}].\end{aligned} \tag{C7}$$

Integrating this expression over the duct cross-section yields

$$\begin{aligned}\bar{P}_z(z_0) = \sum_{m=-\infty}^{\infty}\sum_{\mu=1}^{\infty}\frac{\pi N_{m\mu}^2}{\rho_0 c_0 k}\,\{\mathrm{Re}\,(k_{m\mu})[|A_{m\mu}(z_0)|^2 - |B_{m\mu}(z_0)|^2]\\ +\,2\mathrm{Im}\,(k_{m\mu})\,\mathrm{Im}\,[A_{m\mu}^*(z_0)B_{m\mu}(z_0)]\}.\end{aligned} \tag{C8}$$

with $N_{m\mu}^2$ from equation (A14). The total acoustic power radiated out of the duct can then be computed with

$$\bar{P} = \bar{P}_z(L) - \bar{P}_z(-L). \tag{C9}$$